Edge radial electric field formation after the L-H transition

K. Kamiya

Japan Atomic Energy Agency (JAEA)

December 14 - 18, 2015 School of Nuclear Science and Technology University of Science and Technology of China, Hefei, China

8th International ITER school

Outline

1. **Introduction**
   - ✓ Experimental observations of the radial electric field formation Theoretical predictoins, and comparison with experimental observations.
2. **Key diagnostics (*HIBP and CXRS*)**
3. **Recent experimental results (*JFT-2M*):**
   - ✓ Spatio-temporal structures of the edge Limit Cycle Oscillation (LCO).
   - ✓ Driving Mechanisms for E_r Bifurcation.
4. **Recent experimental results (*JT-60U*):**
   - ✓ Paradigm of E_r-shear suppression of turbulence as the mechanism for the edge transport barrier formation with an improved diagnostic.
   - ✓ Complex multi-stage Er transitions having different time-scales.
   - ✓ Turbulence, transport, and the origin of the radial electric field.
5. **Summary**

Experimental observations of the radial electric field formation after the L-H transition.

First discovery of H-mode plasma in old ASDEX tokamak with divertor (Wagner, PRL 1982).

- Subsequently seen in many medium-sized tokamaks with divertor configuration (e.g. *JFT-2M, PDX/PBX-M, DOUBLET-III/DIII-D, AUG,…*),
- Leading to a standard configuration, including even in the design for large tokamaks (e.g. *JET, JT-60U/SA, and ITER/DEMO*).
- At that time, the *closed* divertor configuration was ***believed*** to be a necessary condition for the H-mode, ***however***, it was reproduced even in limiter and/or open divertor configurations on JFT-2M (Matsumoto, NF 1987).

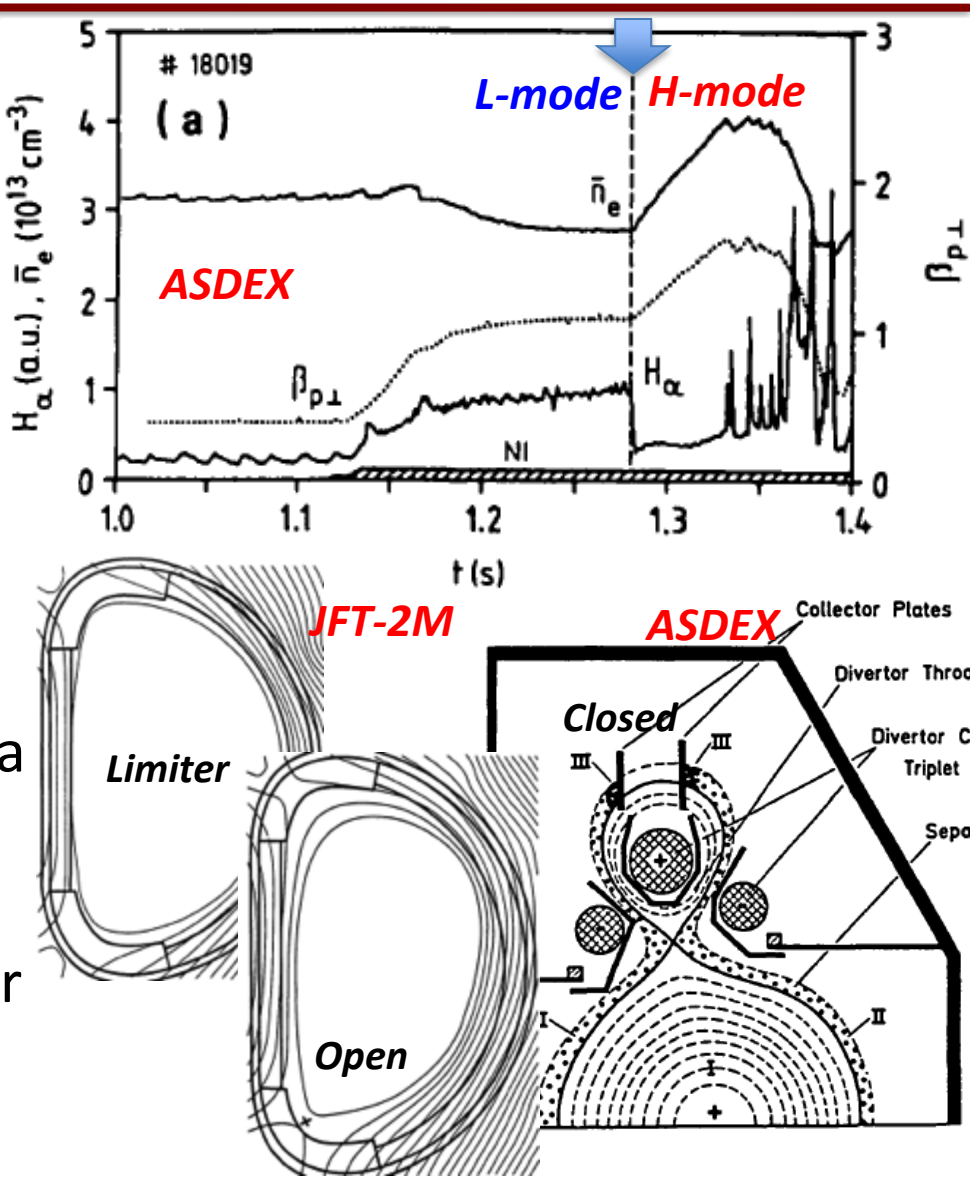

Edge localized E_r structure in H-mode plasma was discovered in DIII-D and JFT-2M, simultaneously.

- According to theoretical prediction, an extensive measurements for the ion density, temperature, and poloidal/toroidal flows at the plasma peripheral region were performed by means of spectroscopic method (CXRS), evaluating the radial electric field;

$$E_r = \nabla p_Z / Z e n_Z - (v_{q,Z} \times B_f + v_{f,Z} \times B_q)$$

Diamagnetic — Poloidal — Toroidal Velocity Term

- After the L-H transition, the E_r and its shear developed in a localized region near the plasma edge.
- Significant reduction in a plasma turbulence level was also seen, althoug exact causality was not yet clear.

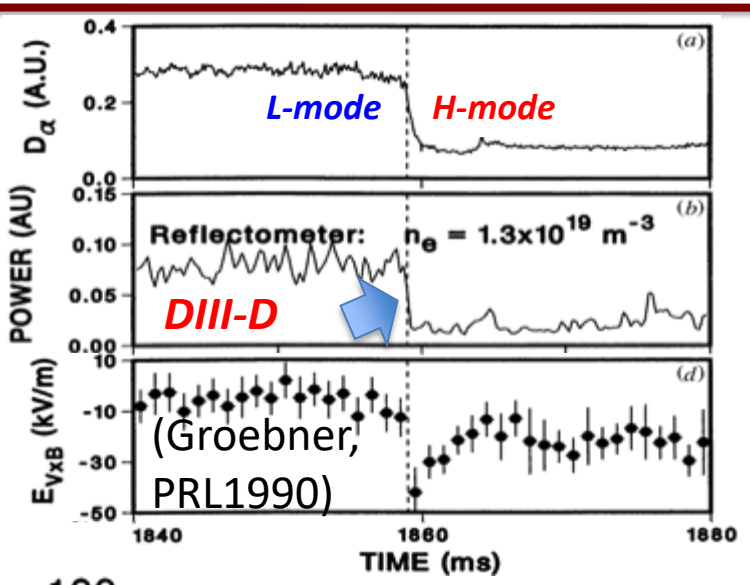

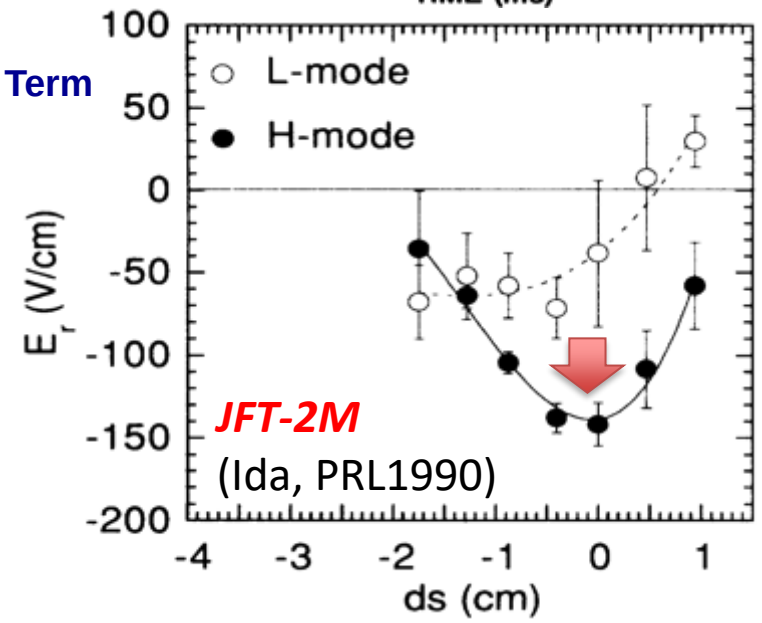

Information on the question of causality was also provided by direct biasing Exp. in CCT plasma

- With biasing, H-mode like transition was demonstrated even in a positive E_r, although poor particle confinement would prevent increase of E_r (negative feedback).

Electric field (positive/negative)

E_r

Turbulence (reduced) $\tilde{n}$ → ∇n Gradient (always negative)

Preventing further increase in positive E_r

- However, the spontaneous transition to the negative E_r can be predicted as seen in many devices, because better particle confinement due to the negative E_r could help further development of negative E_r (positive feedback).

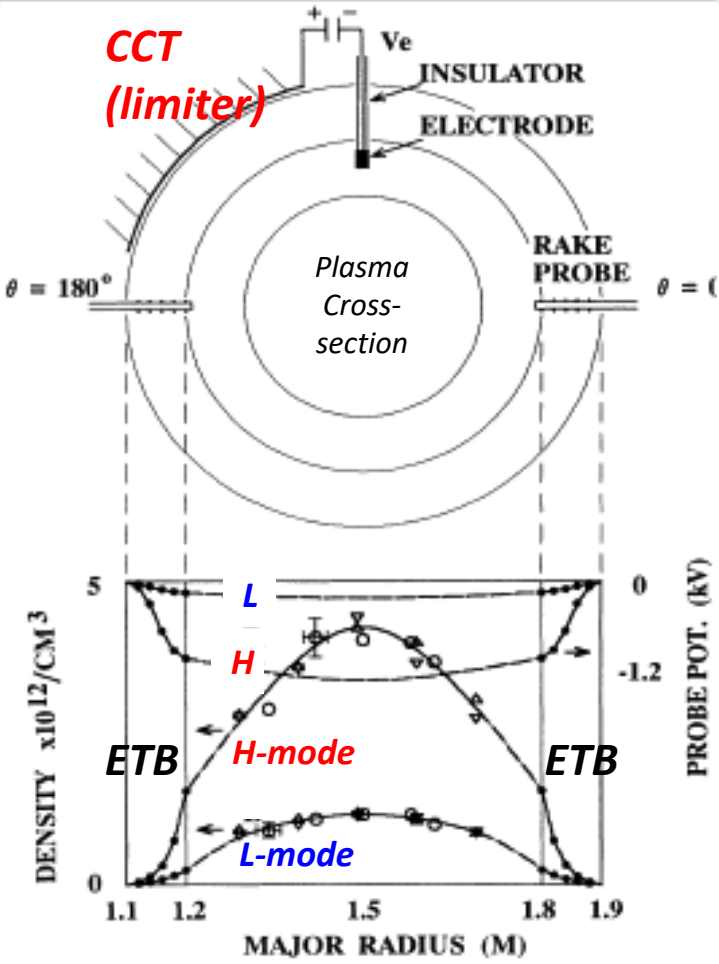

ETB produced by negative biasing in CCT plasma (Taylor, PRL1989).

Direct measurement with fast temporal resolution was performed by a HIBP in JFT-2M

- **The time-scale of the E_r formation at the L-H transition** was found to be 10-100 micro sec (<<tau_E; time-scale for global energy transport).
- Simultaneously, a significant reduction of turbulence intensity and the ETB formation were seen.
- Finally, it became no doubt that the L-H transition should be the transition of the radial electric field as predicted by a theory.
- If so, what is causality for the Er-bifurcation?

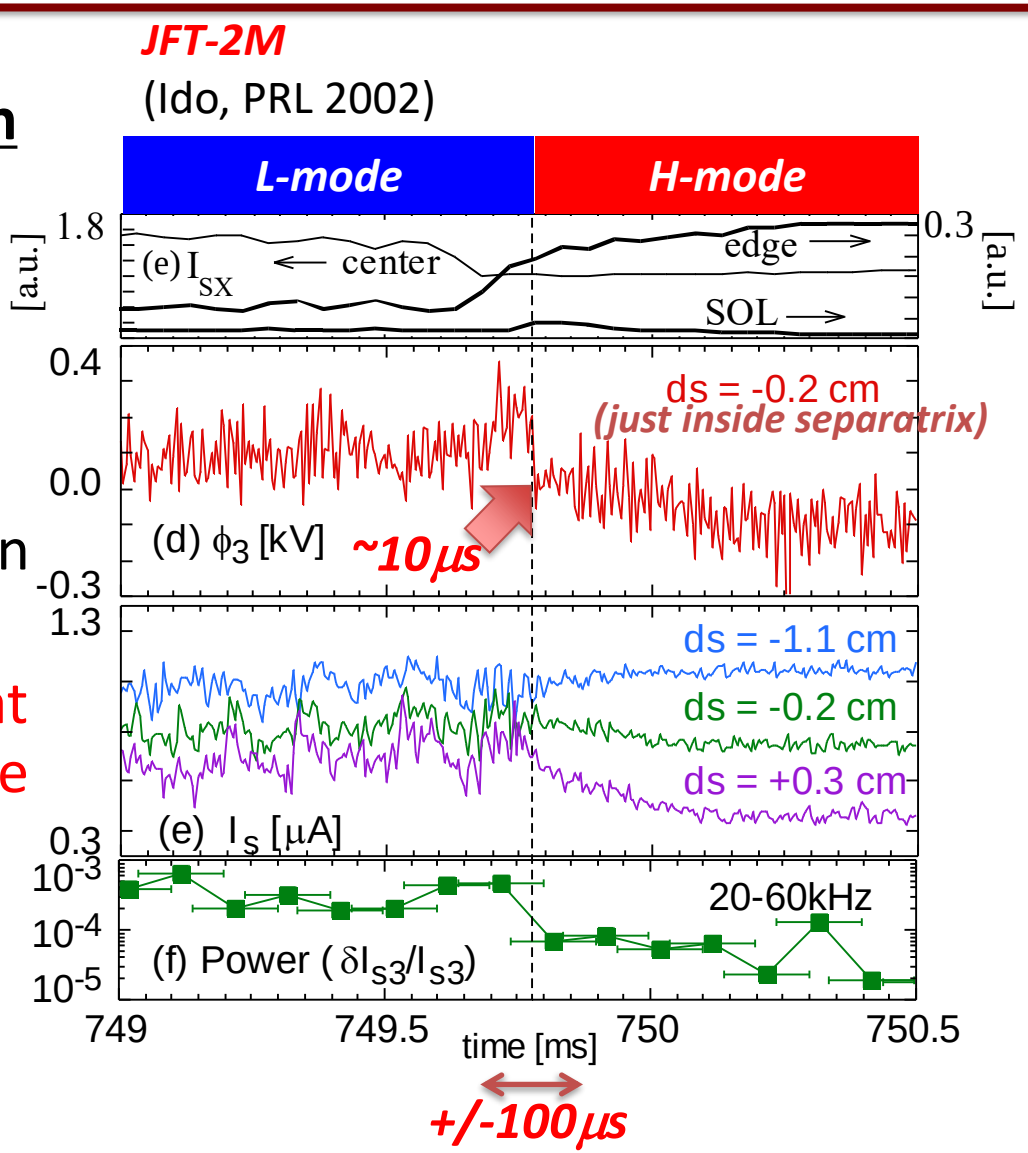

Theoretical study of “poloidal shock” formation, and comparison with experimental observations.

Ion orbit loss model near the plasma boundary was proposed *[Itoh and Itoh, PRL1988]*

- In 1988-89 (>5 years after the 1st H-mode discovery in ASDEX), *before experimental observation*, theoretical work predicted that the E_r might play an important role in the mechanism of the L-H transition.
- Experimental verifications on many devices were also performed [Burrell, PPCF 1992, PoP 1997; Ida, PPCF 1998].
- It is conventionally *believed* that the high confinement regime is achieved when the ***E ×B shear*** is sufficient to stabilize the turbulent fluctuations responsible for anomalously high transport.

Transition from the branch of large flux (L) to small flux (H) occurs at $\lambda=\lambda_C$.

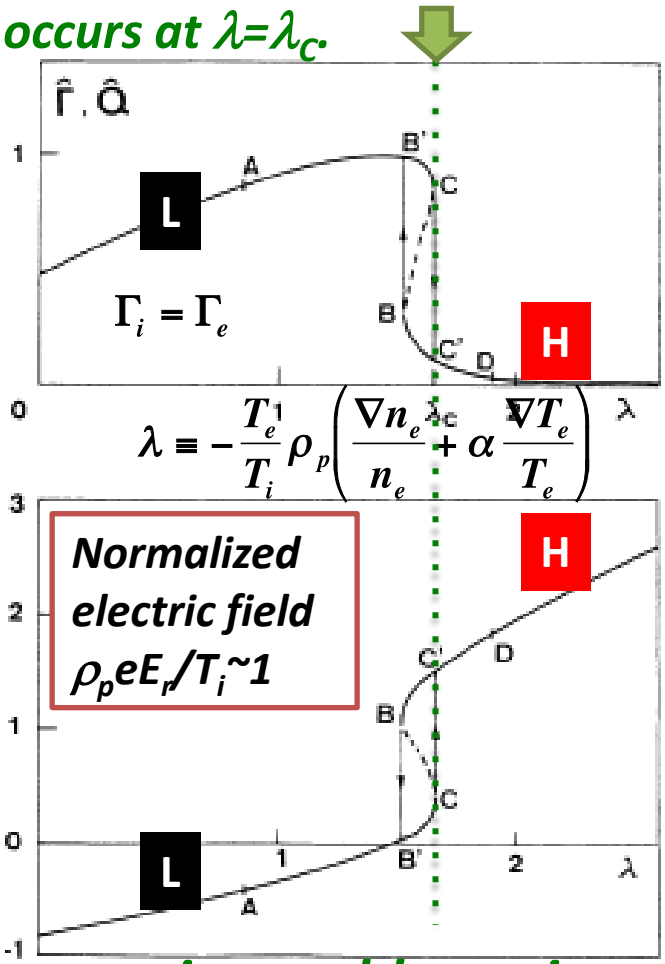

Nevertheless the transition trigger mechanism remains problematic.

Theoretical study in toroidal plasmas had been focused on the poloidal flow formation at high-speed (~*70's*)

The most interesting point was how ***V*** was governed when E_r (=-$\nabla\Phi$) existed, according to the *ideal* ohm's law? $-\nabla\Phi + V \times B = 0$

1) Poloidal flow can be generated due to the coupling with a poloidal non-uniformity in the radial flux (*i.e. Stringer spin-up*). *[Stringer, PRL1969].*

2) Flow structure was categorized by the ***non-dimensional parameter (poloidal Mach number, U_{pm}),*** and "poloidal shock" can be generated at $U_{pm} \approx 1$, depending on the ***normalized ion collisionality***. *[Hazeltine, Phys. Fluids1971]*

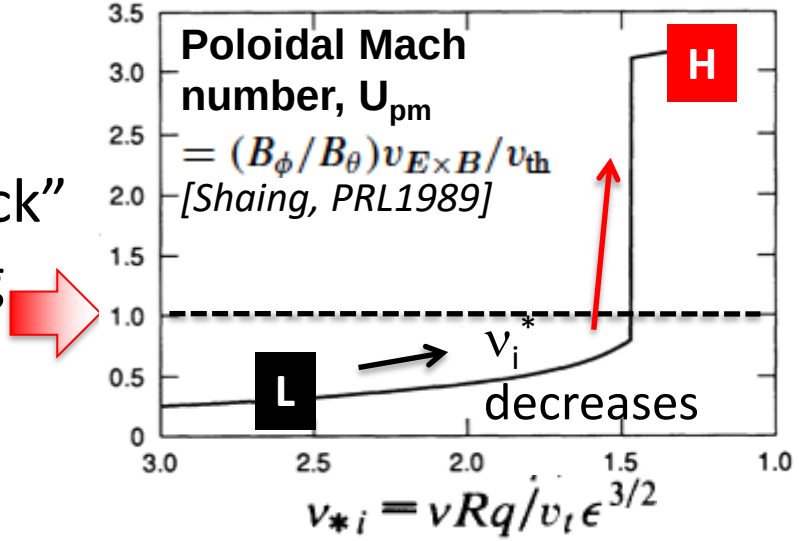

3) In addition to the stationary "mean" flows, oscillating modes (*Zonal flows and/or Geodesic Acoustic Mode*) had been predicted. *[Winsor, Phys. Fluids1968]*

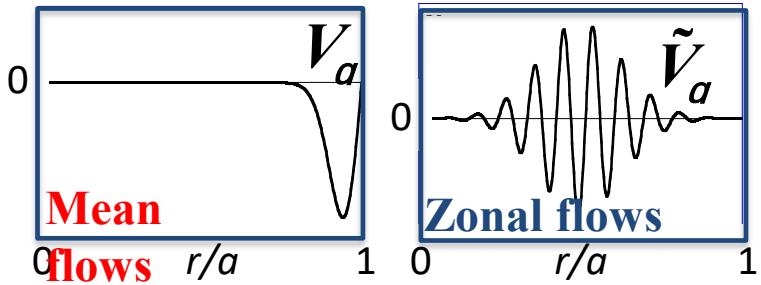

Sequence of the physical events in the L-H transition, according to the ion-orbit loss model

[K. C. Shaing and E. C. Crume, Jr., Phys. Rev. Lett. 63, 2369 (1989).]

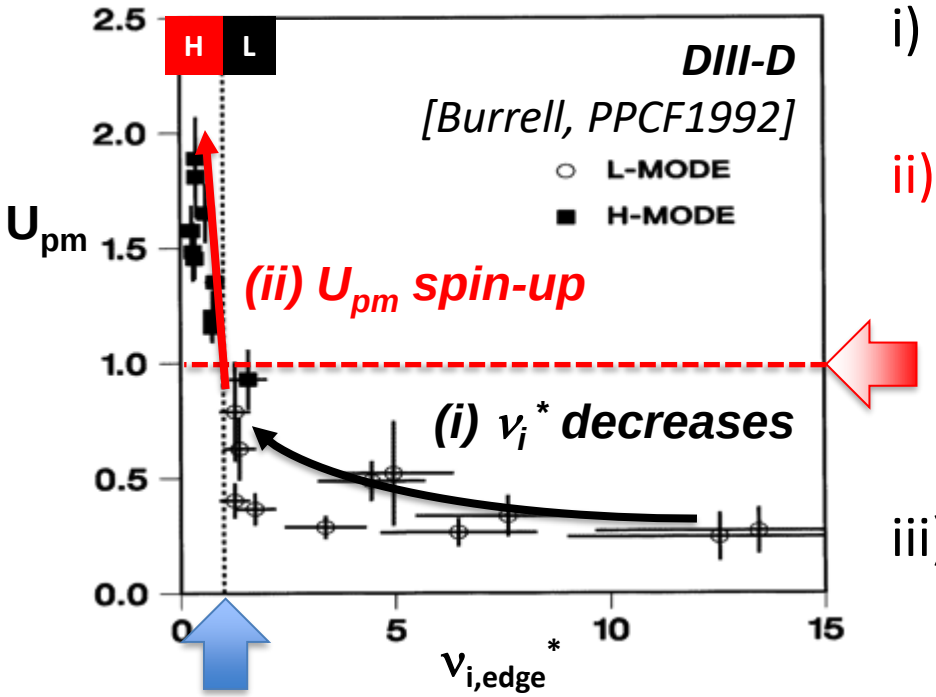

***A critical ν_i^* value**, depending on the details of devices (e.g. hot ion fraction, impurities, neutrals…).*

=> Indeed, larger nyu_i* (=10–50) was reported [Miura, PRL 1992, Carlstrom, PoP 1996]

i) Because of plasma heating, $\nu_{i,edge}^*$ decreases.

ii) U_{pm} makes a transition at a critical value of $\nu_{i,edge}^*$ and becomes more positive [the corresponding E_r value becomes more negative with its time-scale of $\mathbf{O}(\nu_{ii}^{-1})$].

iii) When V_θ increases, fluctuations saturate at lower level due to decrease the de-correlation time for turbulent fluctuations, and the L-H transition thereby occurs.

iV) The D_α intensity drops, and the edge gradient becomes to build in the pedestal …

Rapid changes in the *ion energy distribution* at the transition was observed with the time-of-flight neutral measurement

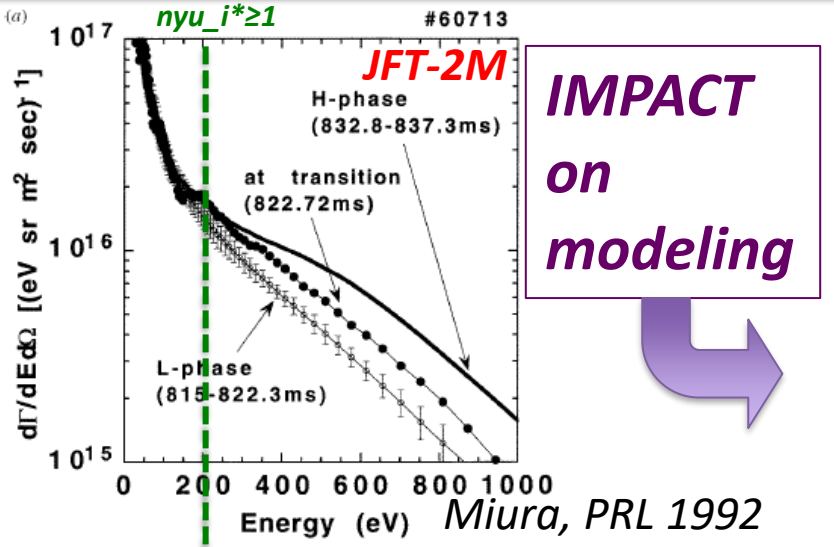

Miura, PRL 1992

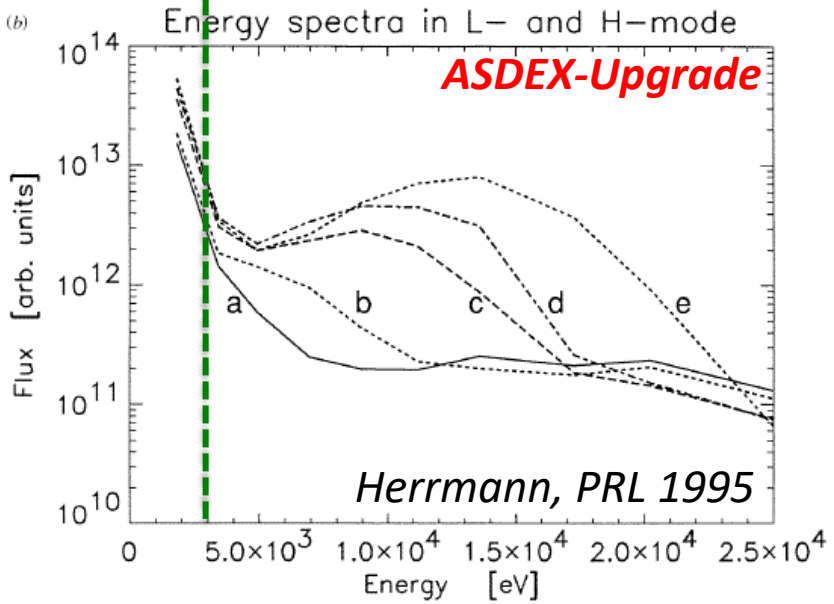

Herrmann, PRL 1995

IMPACT on modeling

- Indeed, the origins that can generate E_r was predicted by theories (Itoh, PPCF 1996).

  Poisson's relation: $\varepsilon_0\varepsilon_\perp \frac{\partial}{\partial t} E_r = e(\Gamma_e - \Gamma_i)$

- The ion loss and the resultant negative E_r seems to one of key mechanisms in L-H transition.
- The deformation of the energy spectrum after the L-H transition implies the squeezing of banana orbit particles due to the E_r (Hinton, PRL 1994).

=> important for dependence of the shear-layer on the poloidal gyro-radius.

Does turbulence Reynolds Stress suffice for an origin of E_r (mean field or ZF) ?

Model: Turbulence transfer free-energy to poloidal flow through the turbulent Reynolds Stress (Kim, PRL 2003, Diamond, PRL 1994, PPCF 2005)

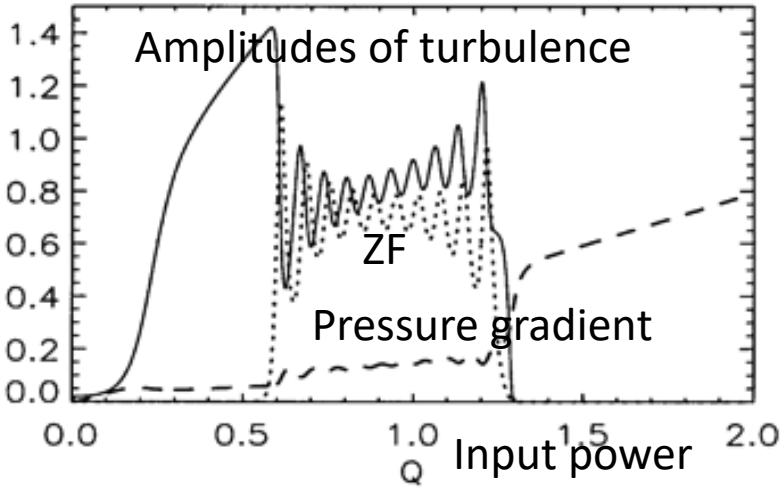

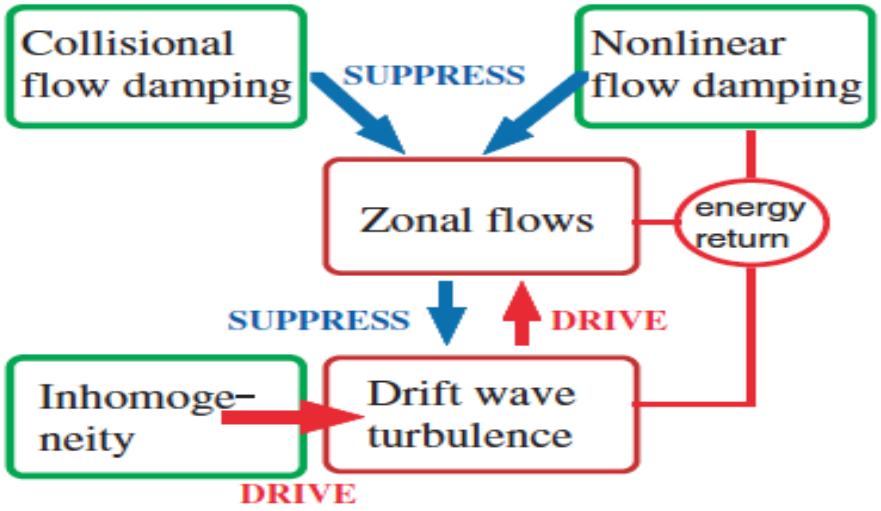

This model is a well-known feature of a predator–prey type dynamical system (widely used in transport barrier formation models).

See. Also Talk by Dr. Gary Staebler at Tuesday Dec 15

Recent observations seem to support the P-P model, but…causality was still unknown due to lack of *direct* E_r measurements.

See. Also Talk by Dr. J. Cheng at Tuesday Dec 15

Experiment: A complex interaction between turbulence driven ExB ZF oscillations (GAMs), the turbulence, and mean flows during the L-H transition (Conway, PRL 2011, Mckee, NF 2009).

Microwave Doppler reflectometry

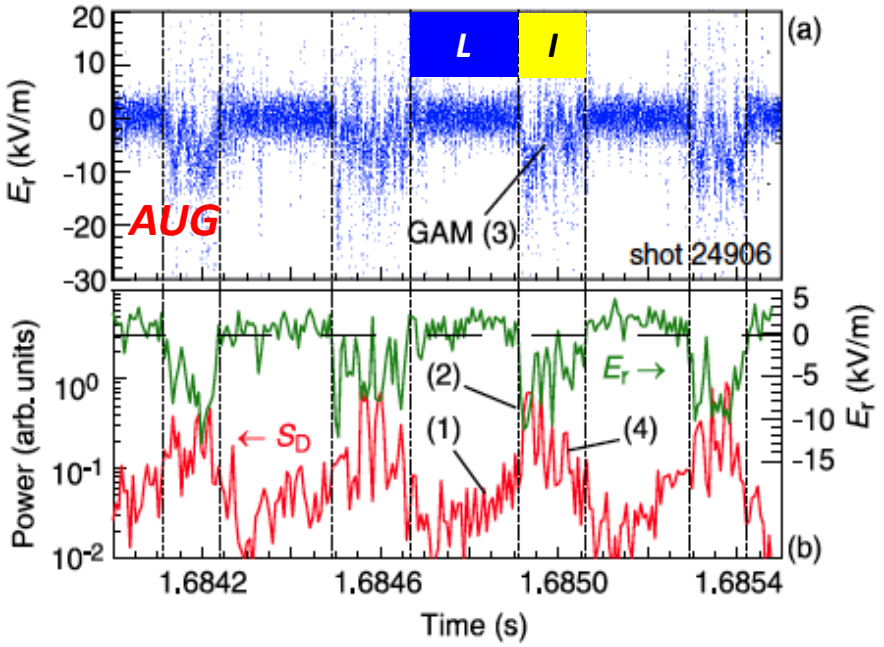

Poloidal turbulence velocity spectrum (BES)

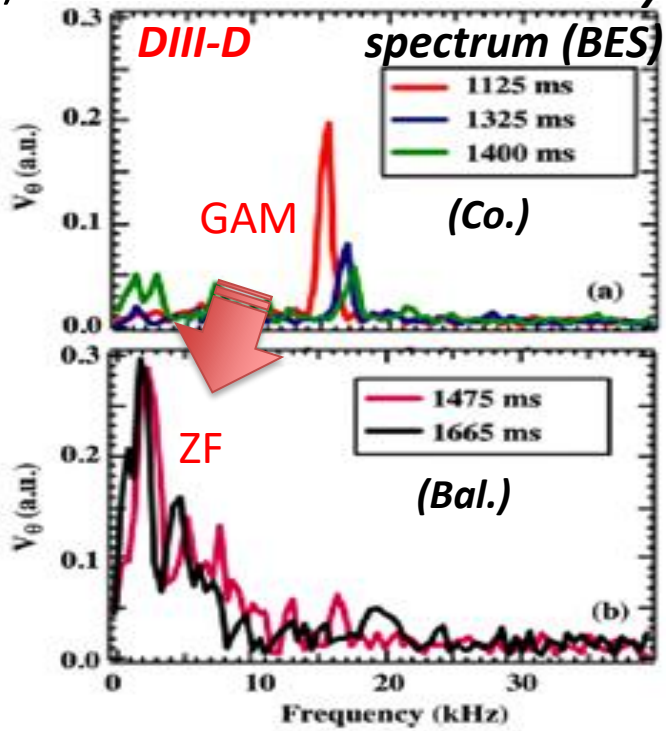

(1) Rising turbulence, (2) threshold, (3) GAM, and (4) turbulence suppression

Transition from GAM to ZF as rotation varies from co-current to bal. during a torque scan.

Key diagnostics

(*HIBP and CXRS*)

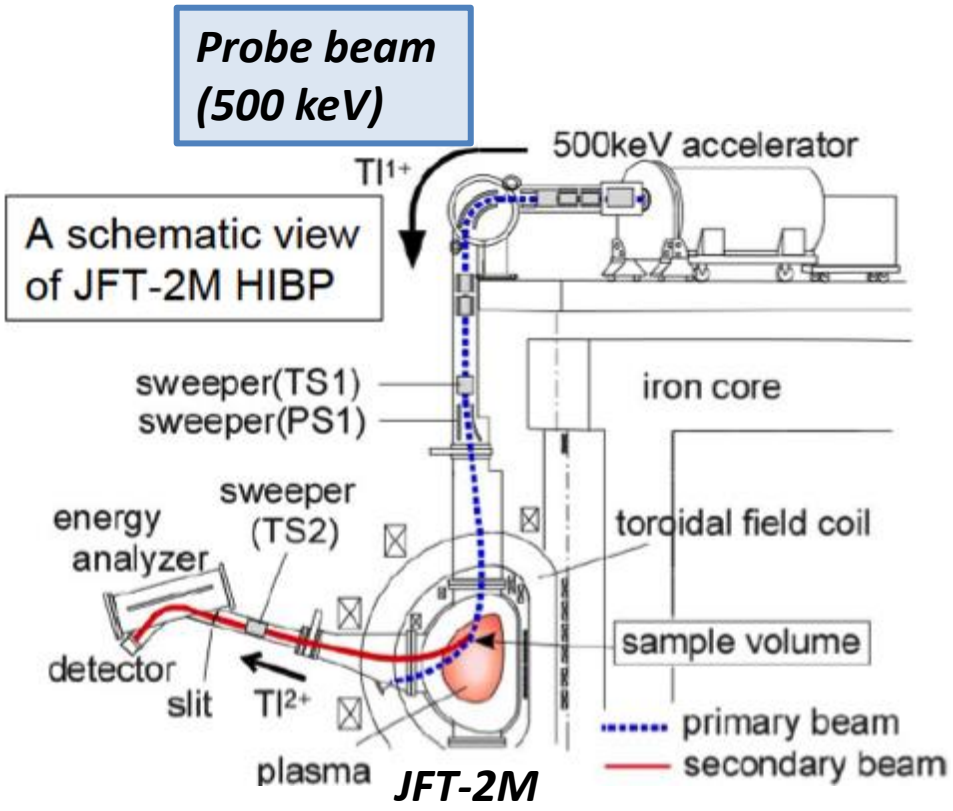

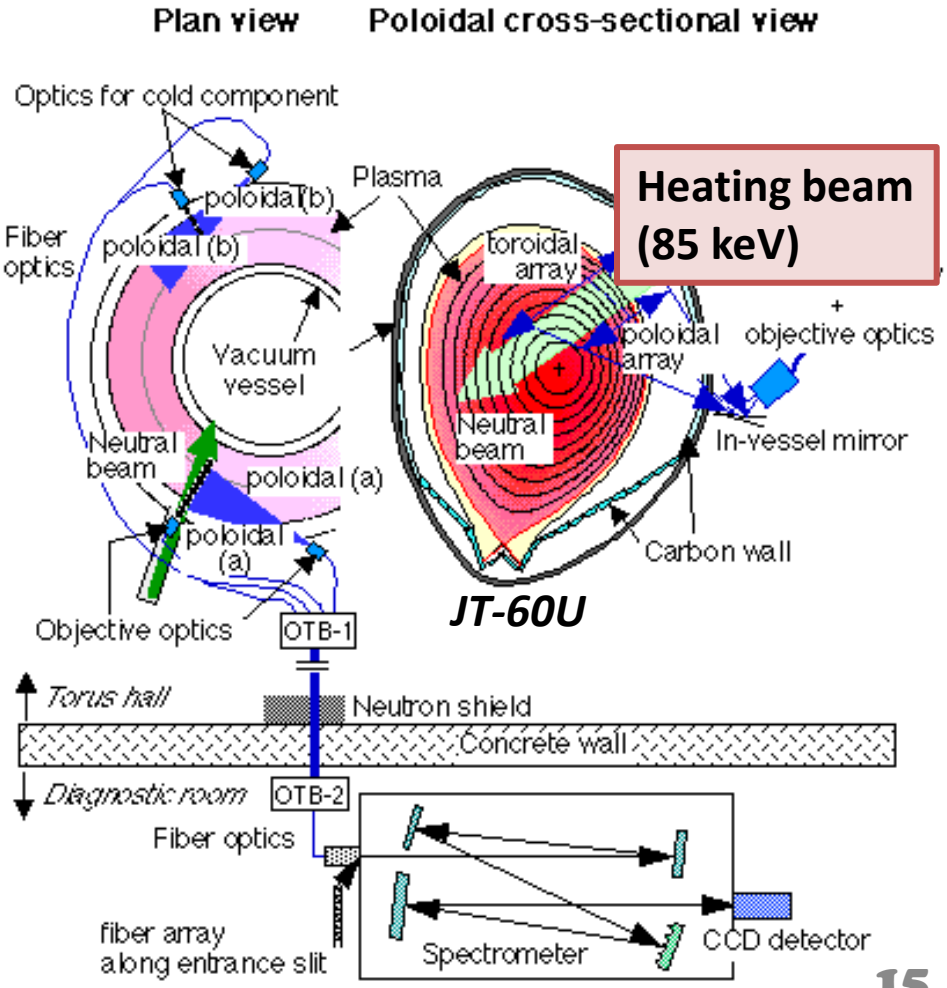

HIBP and CXRS are the most powerful tool for the physics study of edge Er formation during L-H transition

HIBP	CXRS
Direct measurements for the change of potential and fluctuation, simultaneously; $E_r = -\nabla\phi$	Indirect evaluation from radial force balance equation for impurity ions; $E_r = \nabla p_j / Z_j e n_i - V_{\theta,j} B_\phi + V_{\phi,j} B_\theta$
Fast temporal resolution up to 1 micro-sec at a few spatial points, simultaneously, being suitable for the study on causality of ETB formation	***High spatial resolution*** up to ~1 cm at multi-points simultaneously in the pedestal, achieving a better S/N by means of heating neutral beam.
Installation costs is too high (especially for larger devices), depending on the diagnostic beam.	Conventional and useful method in many devices, but time resolution (~1ms, or less) is not enough in some case.
Simultaneous measurement for plasma density fluctuation, but pedestal measurements at higher density is limited due to beam attenuation ($n_e \leq 1\times10^{19}$ m^{-3}, typically).	Even though, CXRS has an advantage for simultaneous measurements of pedestal information (e.g. n_i, T_i, V_p, and V_t).

Recent experimental results *(JFT-2M)*

JFT-2M (JAERI Fusion Torus-2M)

tokamak

R = 1.3 m, a = 0.35 m

$B_t \leq 2.2$ T

$I_p \leq 0.5$ MA

(Medium sized tokamak)

NBI power ≤ 1.6 MW (Balanced)

*Already been shut down in 2004
http://www-jt60.naka.jaea.go.jp/jft2m/

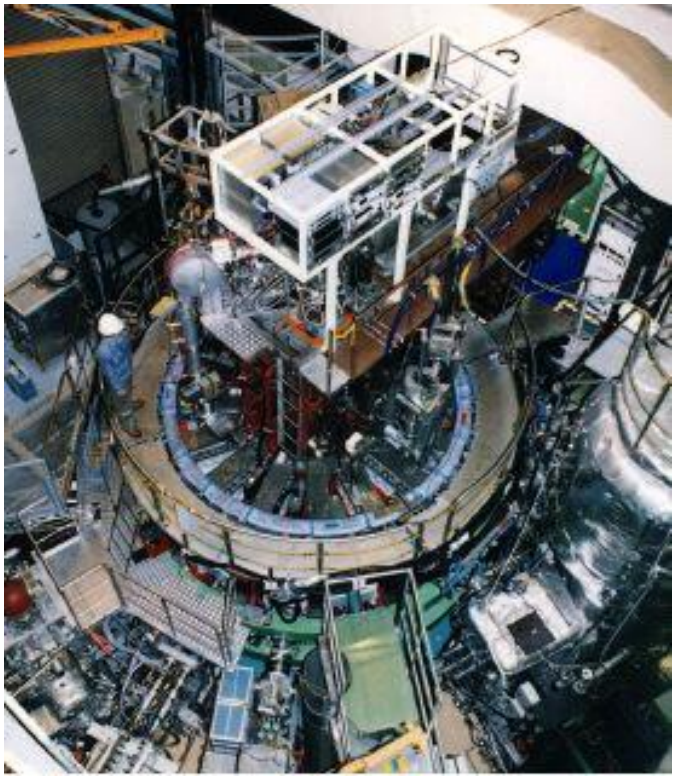

A 500 keV Heavy Ion Beam Probe (HIBP) diagnostic on JFT-2M

JFT-2M

1. Singly charged thallium ions with the accelerated energy of up to 500 keV are injected from the top vertical port.
2. Doubly charged thallium ions are produced due to ionization by the plasma at the localized region.
3. The change in the secondary beam energy due to the plasma potential can be evaluated by using parallel plate energy analyzer with split plate detector.
4. Density and its fluctuation can be evaluated by using beam current estimation; $I_{HIBP}=I_0 A_1 \sigma n_e \Delta l A_2 \approx n_e$

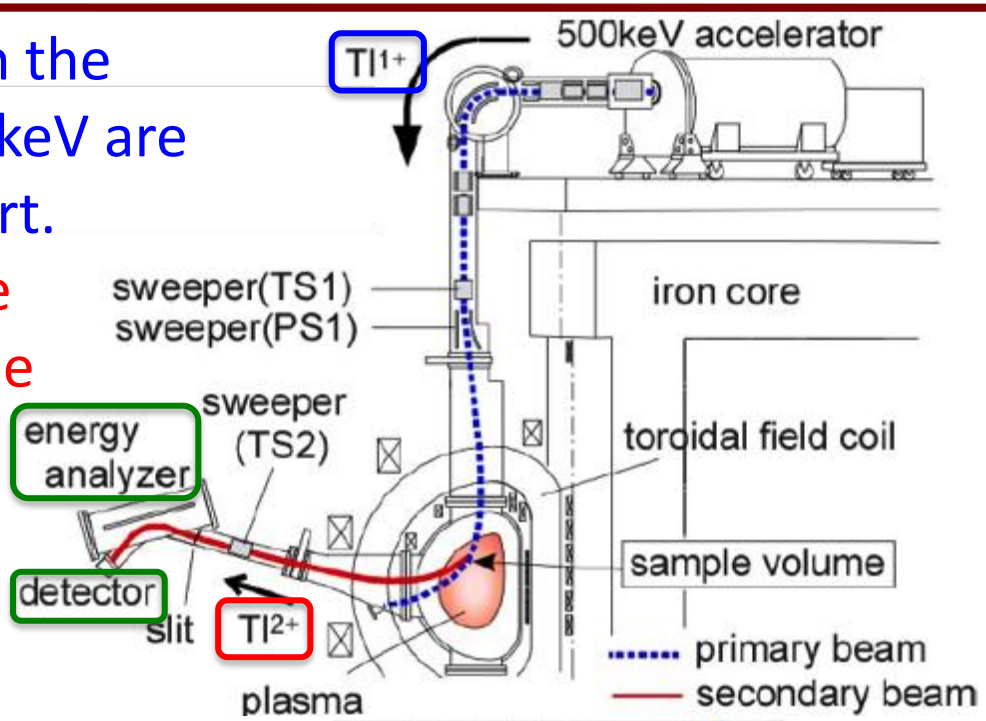

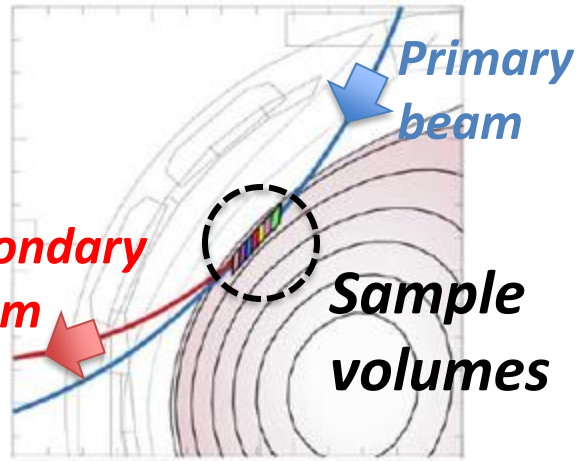

Limit-Cycle Oscillation (LCO) was seen just before the L-H transition on many devices

Kobayashi, PRL 2013

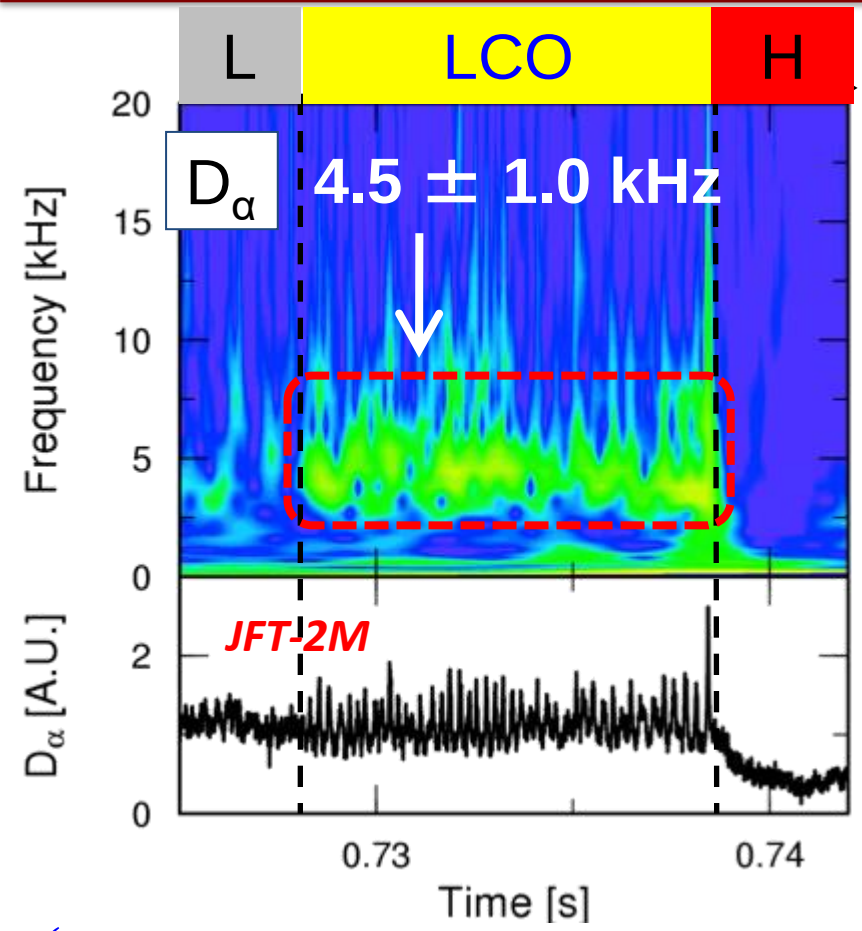

- ✓ Theoretical models [Itoh-Itoh, PRL 1991; Kim-Diamond PRL 2003].
- ✓ Experimental observations (TJ-II, and AUG, DIII-D, EAST, HL-2A, …).

- However, understanding of the physical mechanism is still not be completed due to lack of ***direct measurements*** for the E_r,…
- Because of difficulties for simultaneously multi-channeled measurements for determination of ZF (*e.g. Analogy from Doppler reflectometory and/or floating potential measurement by probe*).
- HIBP is powerful-tool to explain the physical mechanism of the LCO, and hence we revisited this study in JFT-2M with HIBP.

Theoretical models that could explain LCO.

Model-1: E_r bifurcation

S-I. Itoh, K. Itoh et al., PRL **67**, 2485 (1991)

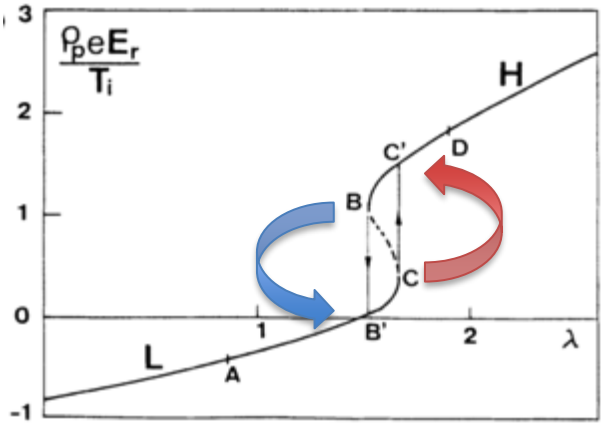

- LCO can be explained as a transition between two overlapped possible E_r values, by changing the *non-ambipolar radial flux*.
- Basically, LCO is dynamics among turbulence, mean pressure, and mean electric field.

$$\frac{\varepsilon_0\varepsilon_\perp}{e}\frac{\partial}{\partial t}E_r = \Gamma_{e-i}^{\text{anom}} - \Gamma_i^{\text{lc}} - \Gamma_i^{\text{bv}} - \Gamma_i^{v\nabla v} - \Gamma_i^{\text{cx}} - \Gamma_i^{\text{NC}} + \Gamma_e^{\text{NC}}$$

Model-2: Predator-prey model

Kim & Diamond: PRL **90** 185006 (2003)

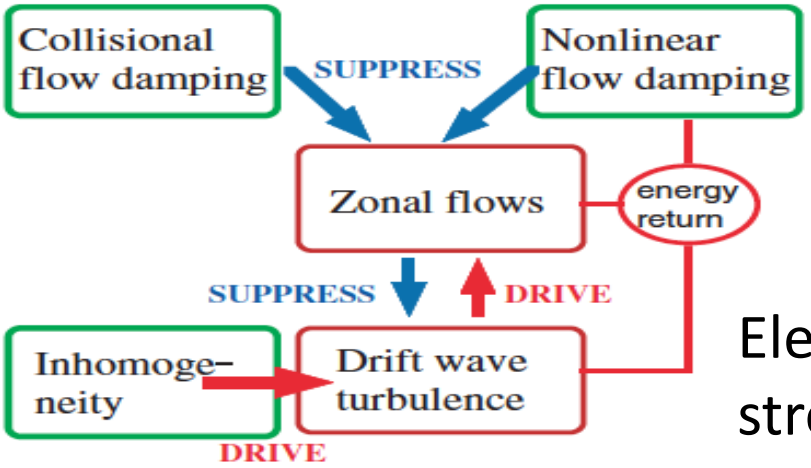

1. Turbulence intensity increases, and that excite ZF.
2. Excited ZF suppresses the turbulence.
3. ZF is also decay because the energy source (turbulence) no longer exists.

Electric field excitation process is Reynolds stress driven.

$$\varepsilon_\perp \frac{\partial}{\partial t} V_\theta = -\nabla\langle \tilde{v}_r \tilde{v}_\theta \rangle - \nu_{\text{damp}} V_\theta$$

Mean profile of E_r and density gradient in both L-mode and LCO phases are found to be similar

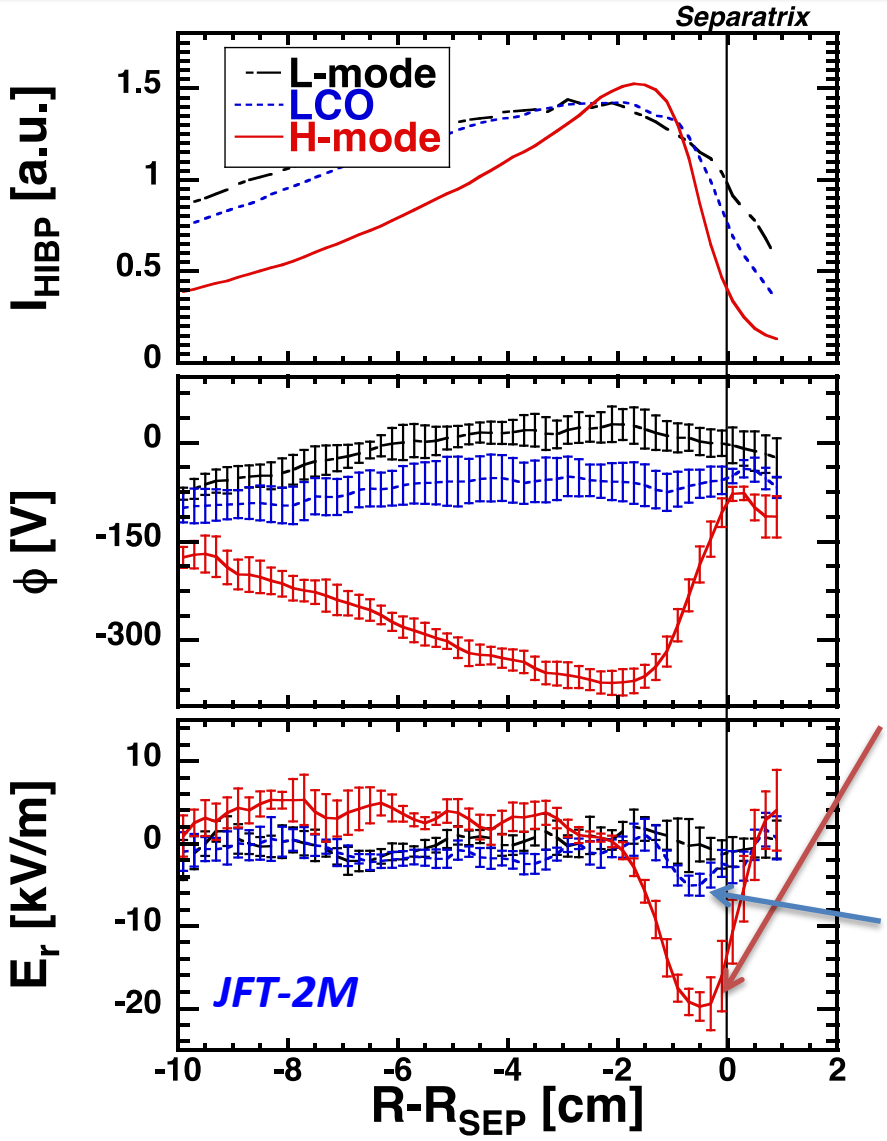

H-mode;

- ✓ Steep gradient in I_{HIBP} (density gradient becomes steeper)
- ✓ Strong E_r (=-dϕ/dr)

E_r × B velocity (~ 30 km/s) is quite larger, in comparison with the amplitude of the flow modulation induced by the LCO (~0.5 km/s)

Micro-scale turbulence in LCO phase was also similar to that in L-mode

JFT-2M

Power spectrum of φ

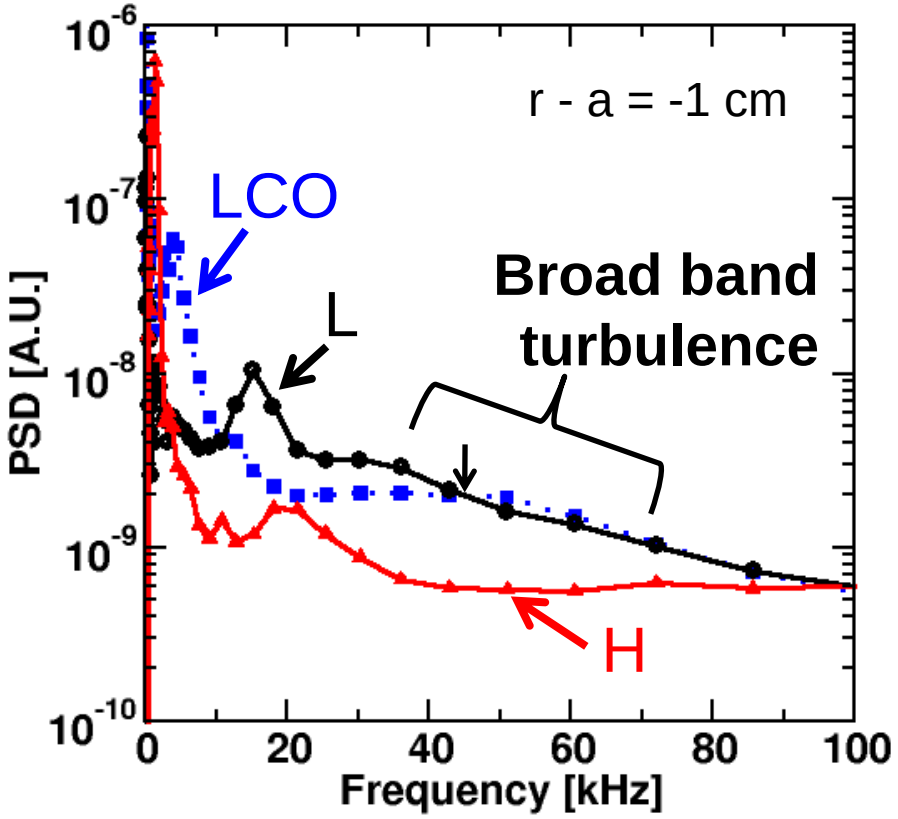

In H-mode, high frequency component is suppressed.

(*Kobayashi, PRL 2013, NF2014*)

⇒Family of drift wave

- m ~ -20 (electron dia.)
- Phase difference; $\tilde{N} \sim e^{-i0.4\pi e\tilde{\phi}/T_e}$
- $\omega/k_\theta \sim V_{d,e}=T_e/(eB_tL_n)$~4 km/s

$(\text{i.e., } k_\theta \sim -0.7 \pm 0.1 \text{ cm}^{-1})$

(Averaged in LCO period)

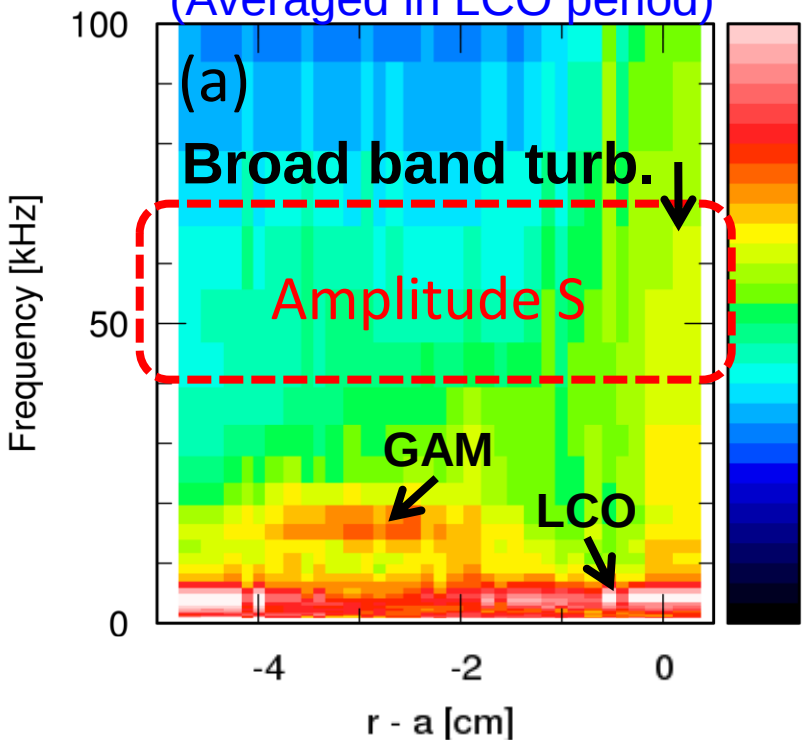

Spatio-temporal structure of φ and density fluctuations during LCO phase

Potential fluctuation: φ

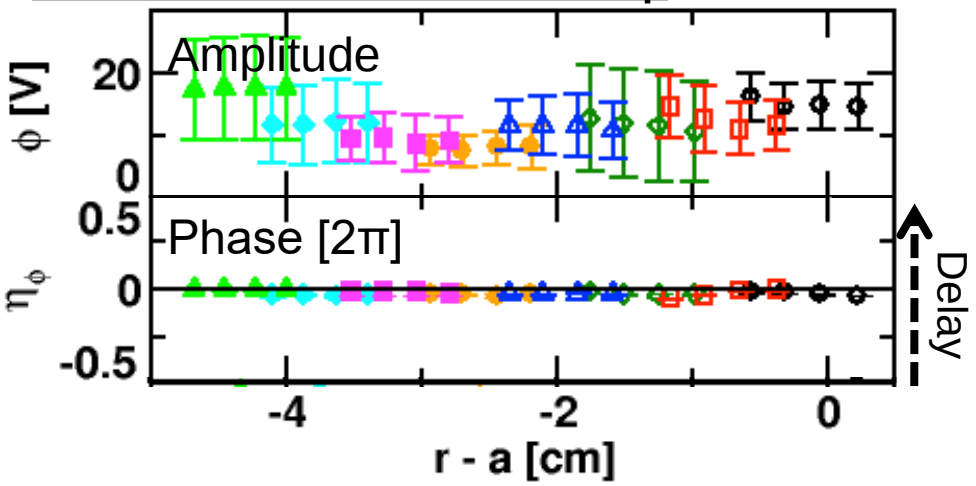

Density fluctuation: N

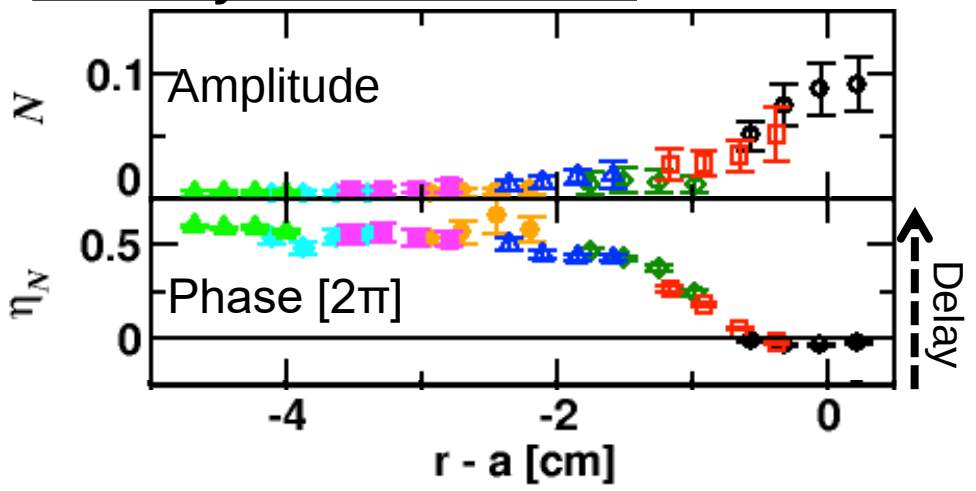

- Amplitude has homogeneous profile for LCO (f~4.5 kHz)
- Phase difference ~ 0
  → k_r~0 (*Not* zonal flows)

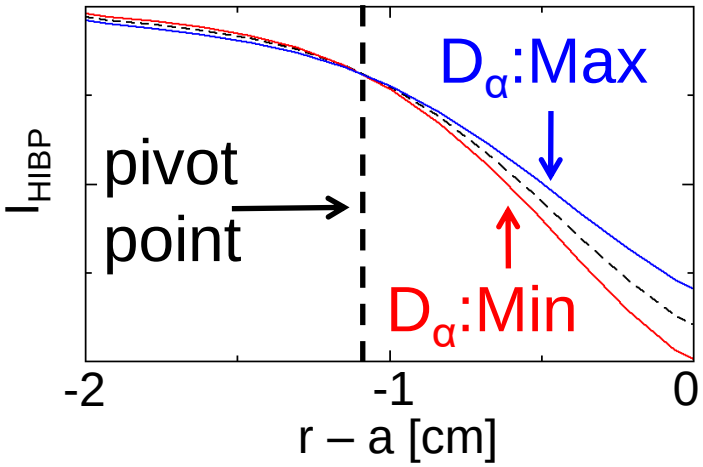

- A peak at r-a ~ 0 cm
- Phase inversion at r-a ~ -1 cm

→Small ETB formation and crash during LCO.

JFT-2M (*Kobayashi, PRL 2013, NF2014*)

Reynolds stress drives only ~15 m/s of poloidal velocity modulation during LCO

JFT-2M

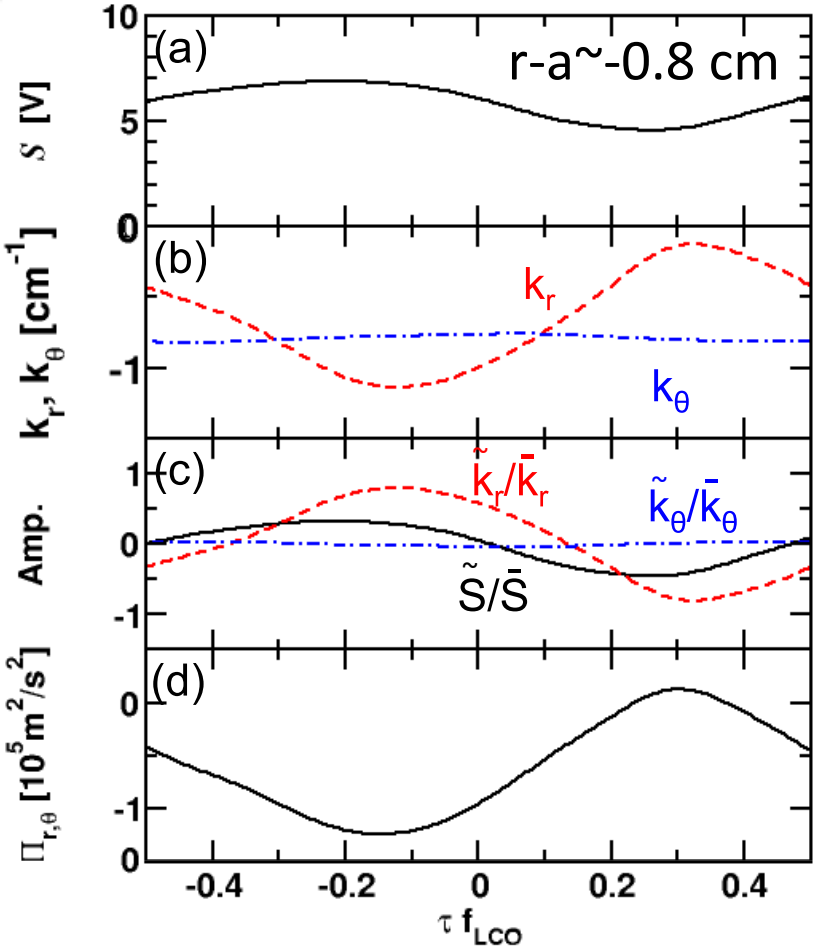

(conditional average of 21 oscillation periods)

Reynolds stress (f=40-70 kHz)

$$\Pi_{r\theta} = \langle \tilde{E}_r \tilde{E}_\theta \rangle / B^2$$

$$= -S^2 k_r k_\theta / (2\,B^2)$$

$$\hat{\Pi}_{r\theta} = -\bar{S}_0^2 \bar{k}_r \bar{k}_\theta \{2\hat{S}/\bar{S} + \hat{k}_r/\bar{k}_r + \hat{k}_\theta/\bar{k}_\theta\} / (2\,B^2)$$

Equation of motion

$$\epsilon_\perp \partial \hat{V}_{E\times B}/\partial t = \partial \hat{\Pi}_{r\theta}/\partial r + \cdots$$

where, dielectric constant: $\epsilon_\perp = 1 + 2q^2$ ~20

Evaluated flow modulation is:

$$\delta|\hat{V}_{E\times B}| \sim |\hat{\Pi}_{r\theta}| L^{-1} \epsilon_\perp^{-1} \omega_{LCO}^{-1} \sim 15 \text{ m/s}$$

ExB flow modulation ~500 m/s.

Small role of turbulence in poloidal acceleration is consistent with the observation that the oscillatory flow in LCO is not zonal flows.

Discussion: Causal Relation among Electric Field E_r, Turbulence S and Density gradient L_n^{-1}

JFT-2M

at the location of maximal E_r amplitude during LCO.

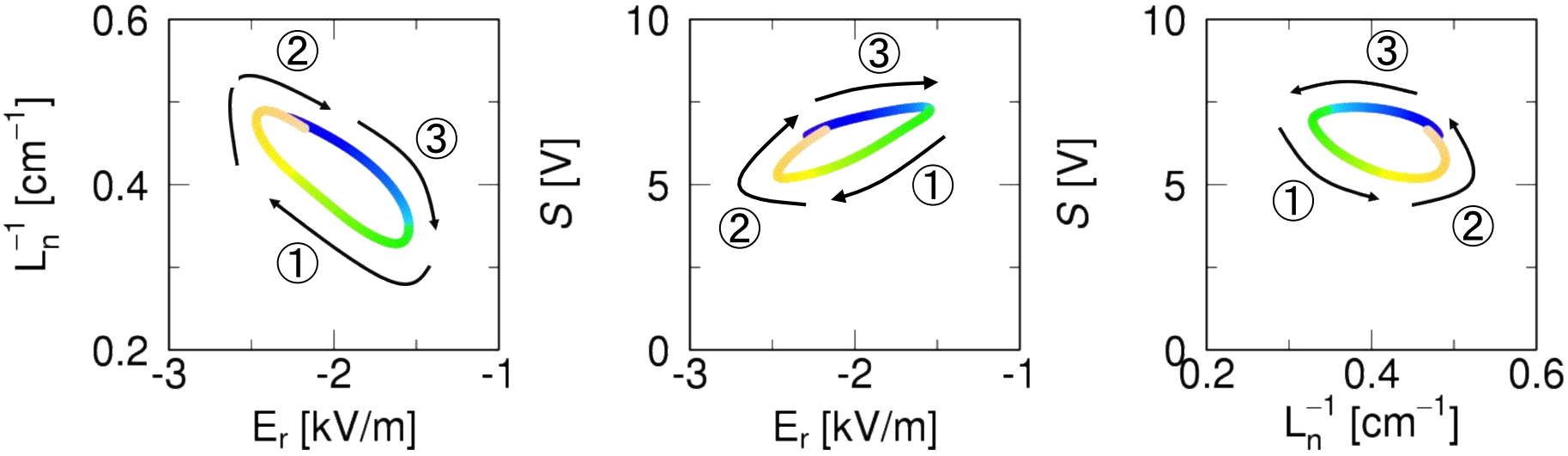

(1) Growth of $-E_r$ suppresses S and transport, and induces the growth of L_n^{-1}.

(2) Strong L_n^{-1} excites S and transport.

(3) Transport leads to decay of $-E_r$ and following relaxation of L_n^{-1}.

Observed temporal evolution seems to be corresponds to the E_r bifurcation model [S.-I. Itoh, K. Itoh., et al., PRL (1991)],

=> Perhaps, the E_r-bifurcation model may maintain the LCO phases, rather than P-P model.

Recent experimental results (*JT-60U*)

JT-60U (JAERI tokamak 60 m^3 upgrade)

R = 3.4 m, a = 1 m

$B_T \leq 4$ T

$I_P \leq 3$ MA

(Large sized tokamak)

NBI power ≤ 40 MW

*Already been shut down in 2008, aiming for the establishment of JT-60SA

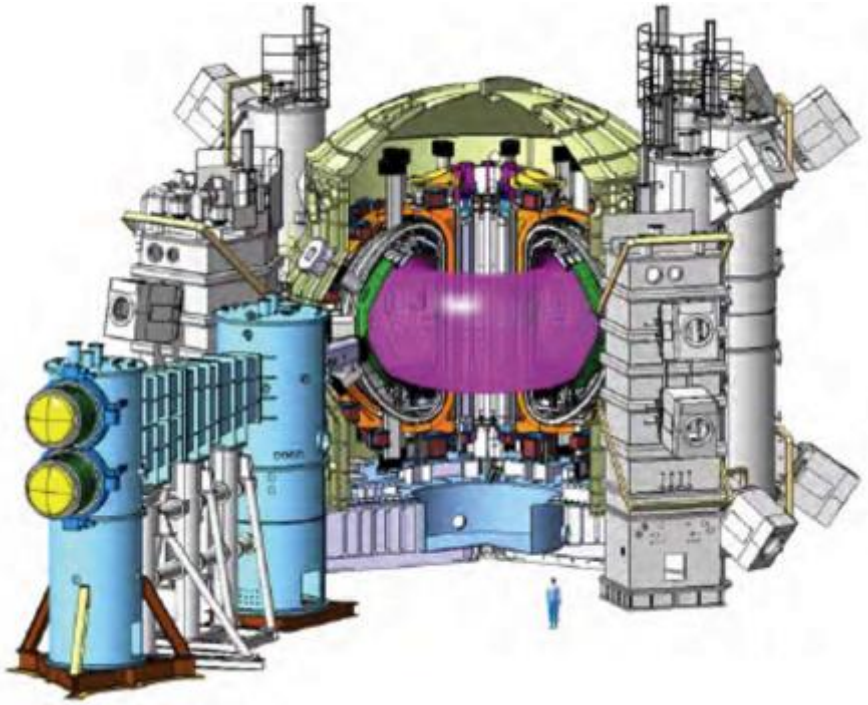

http://www-jt60.naka.jaea.go.jp

E_r and its associated shear play a key role for the plasma turbulence and transport

- L-H transition could be related to the ***E_r bifurcation*** at the plasma edge region as *predicted by a theory* [*H. Biglari, Phys. Fluids 1990, S.-I. Itoh, PRL1994*].
- ***E_r-shear stabilization*** effects on the transport barrier formation seen in many deices, although exact causality seems to be still unclear [*e.g. P_{TH}=f(x), Hydrogen-isotope effects,…*].
- Furthermore, the effect of ***E_r-curvature*** on the turbulence suppression is also important for considering the *nonlinear effects* (e.g. radial squeezing or broadening of the turbulent eddies) [*K. Itoh and S.-I. Itoh, PPCF 1996, P. Diamond, PPCF2005*].

=>> It needs a more detailed experimental and theoretical validation based on a high-resolution measurements with a better S/N.

Shear and *Curvature* of Electric Field
(Which is more important, and how?)

Shear and enhanced nonlinear damping

K. Itoh, talk at PET 2015

The circular element of the vortex is stretched after the elapse of time

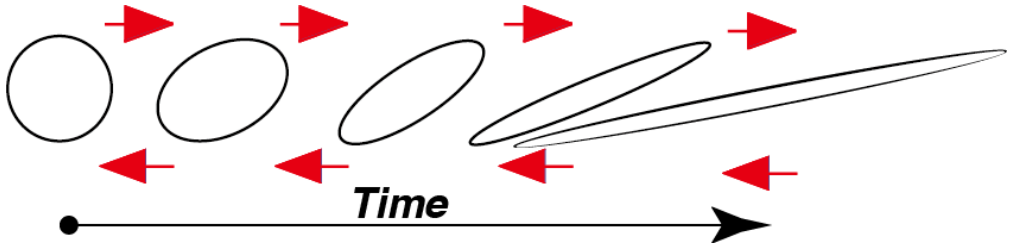

The sheared average flow distorts the turbulent eddies, leading to decorrelation between the density and velocity perturbations.

Curvature and drive of a flow

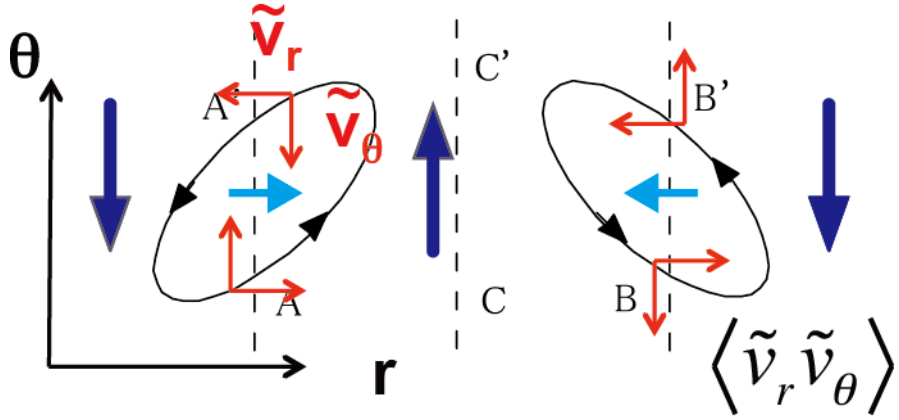

Suppression of microscopic fluctuations via modulational coupling

Theoretical prediction of the turbulence intensity;

$$I/I_0 = 1 + \alpha (E_r')^2 + \beta E_r E_r''$$

==> Determining the proportionality coefficients should be a remaining issue for both theoretical and experimental work.

[1] H. Biglari, Phys. Fluids B **2** (1990) 1
[2] S.-I. Itoh, et al., Phys. Rev. Lett. **72** (1994) 1200
[3] K. Itoh and S.-I. Itoh, Plasma Phys. Contr. Fusion **38** (1996) 1–49
[4] P. H. Diamond, et al., Plasma Phys. Contr. Fusion **47** (2005) R35-R161

Diagnostic

JT-60U ELMy H-mode plasmas with balanced NBI heating

$$E_r = \nabla p_Z / Zen_Z - (v_{q,Z} \times B_f + v_{f,Z} \times B_q)$$

Diamagnetic | Poloidal | Toroidal Velocity Term

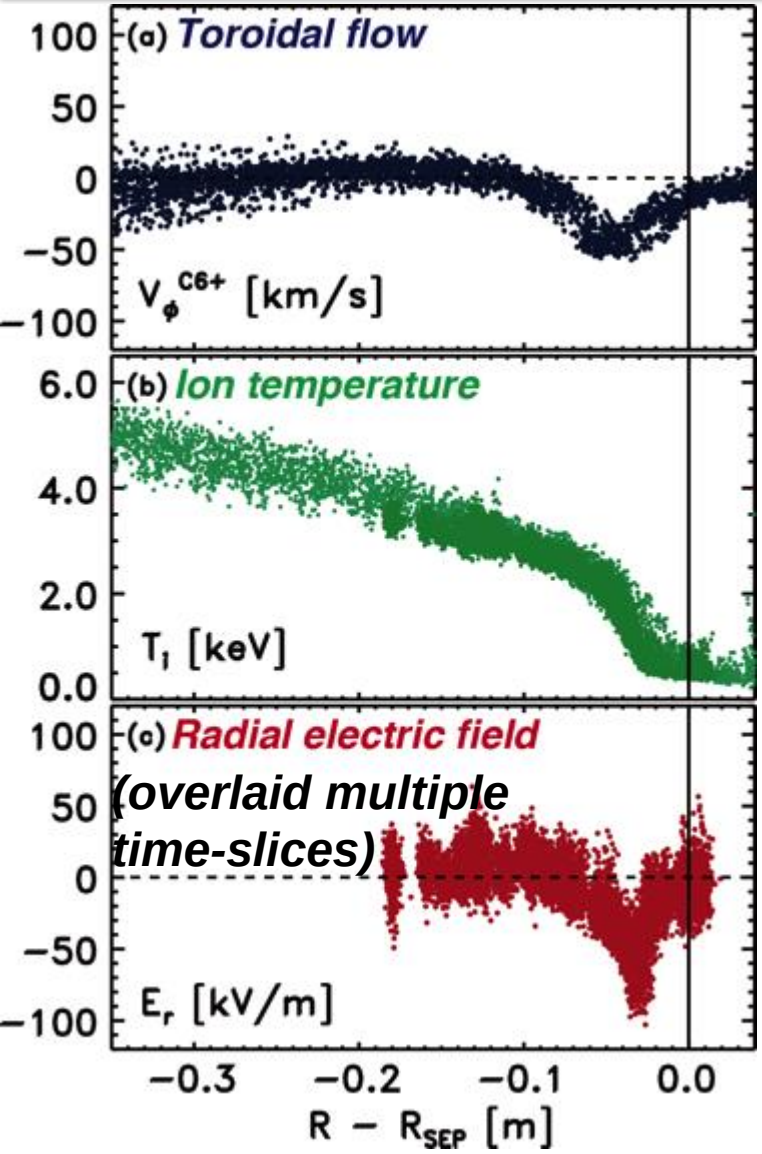

- On JT-60U, we measured the radial profiles for the n_i, T_i, V_{pol}, and V_{tor} for the C^{6+} using ***CXRS*** *diagnostic* with fast time resolution (up to 400 Hz) at 59 spatial points (23 tor. and 36 pol. viewing chords).
- With regard to determining the $E_r(r)$, we apply a novel diagnostic for the V_{tor} having higher spatial resolution, in addition to the conventional one.

CXRS (Conventional) ***[Koide, RSI 2001]***

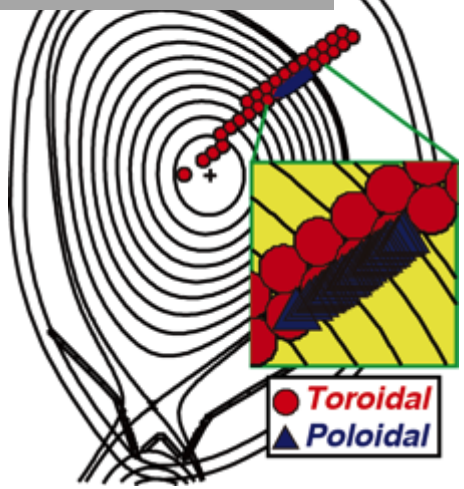

Modulation CXRS ***[Ida, RSI 2008]***

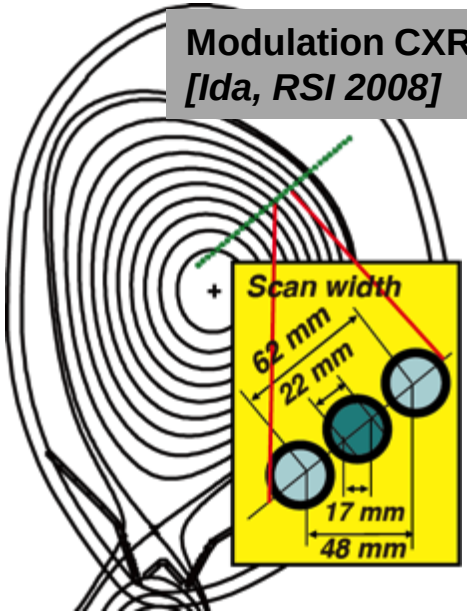

Shot comparison overview

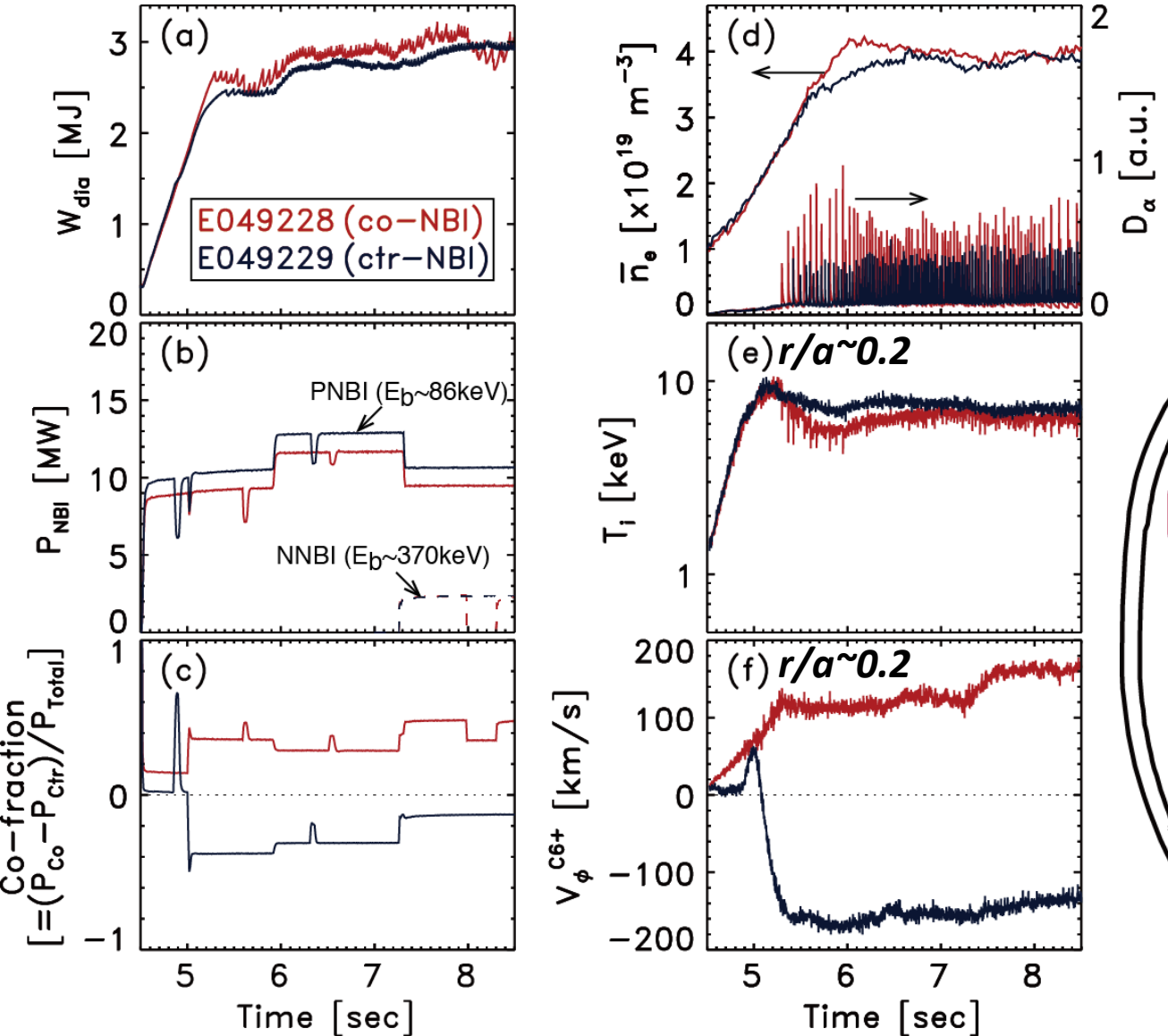

I_p/B_T=1.6MA/3.8T
(q_{95}~4.2)
κ/δ=1.47/0.36
(V_{plasma}~57 m^3)

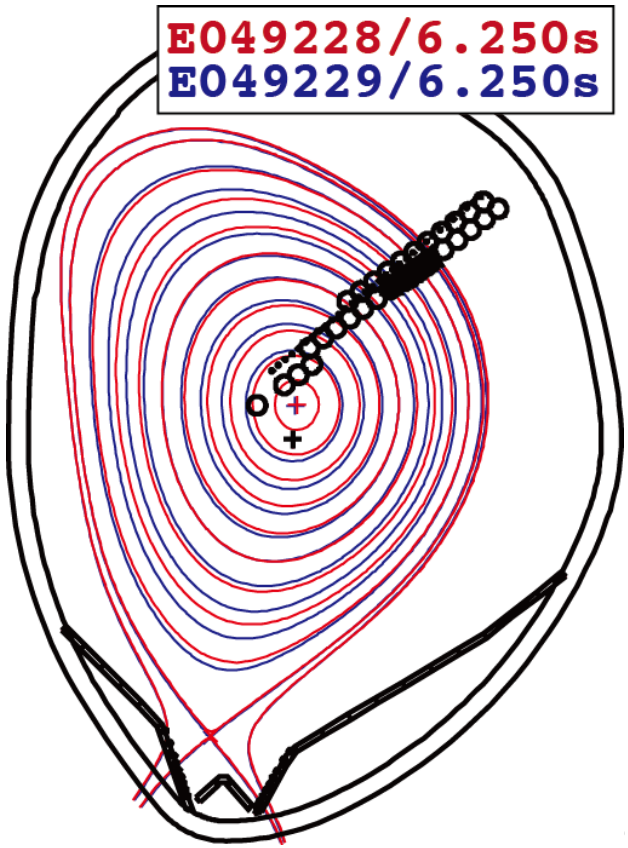

Improved statistics in assessing the temporal behavior of the measurements can be obtained

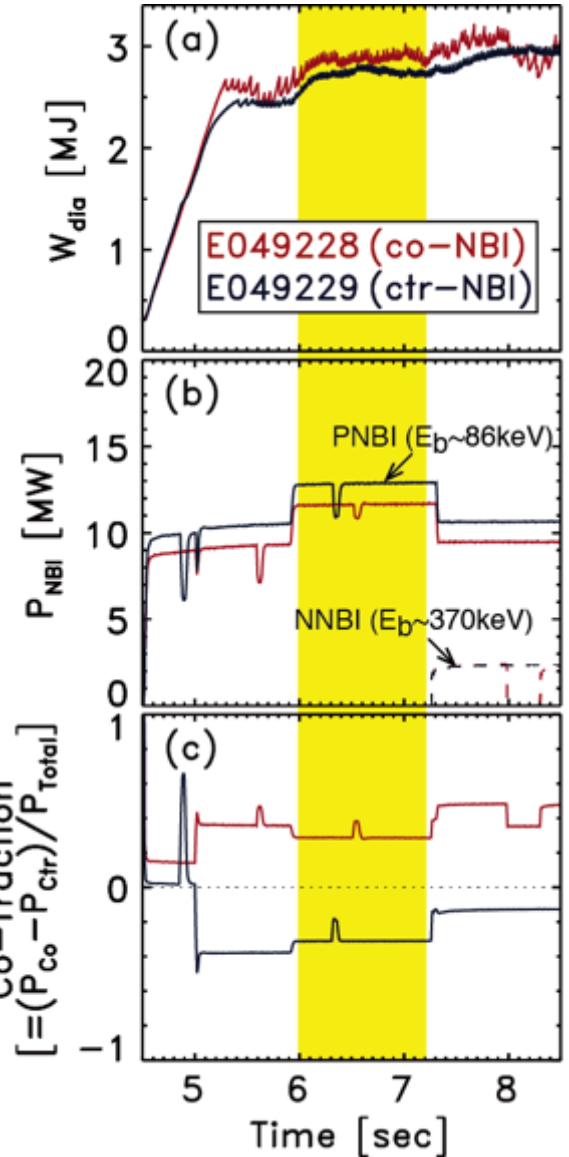

Co.: f_{ELM} = 33.2 [Hz], $\Delta W_{ELM}/W_{ped.}$ = 9.3 [%]
Ctr: f_{ELM} = 40.1 [Hz], ($\Delta W_{ELM}/W_{ped.}$ = 6.1 [%])

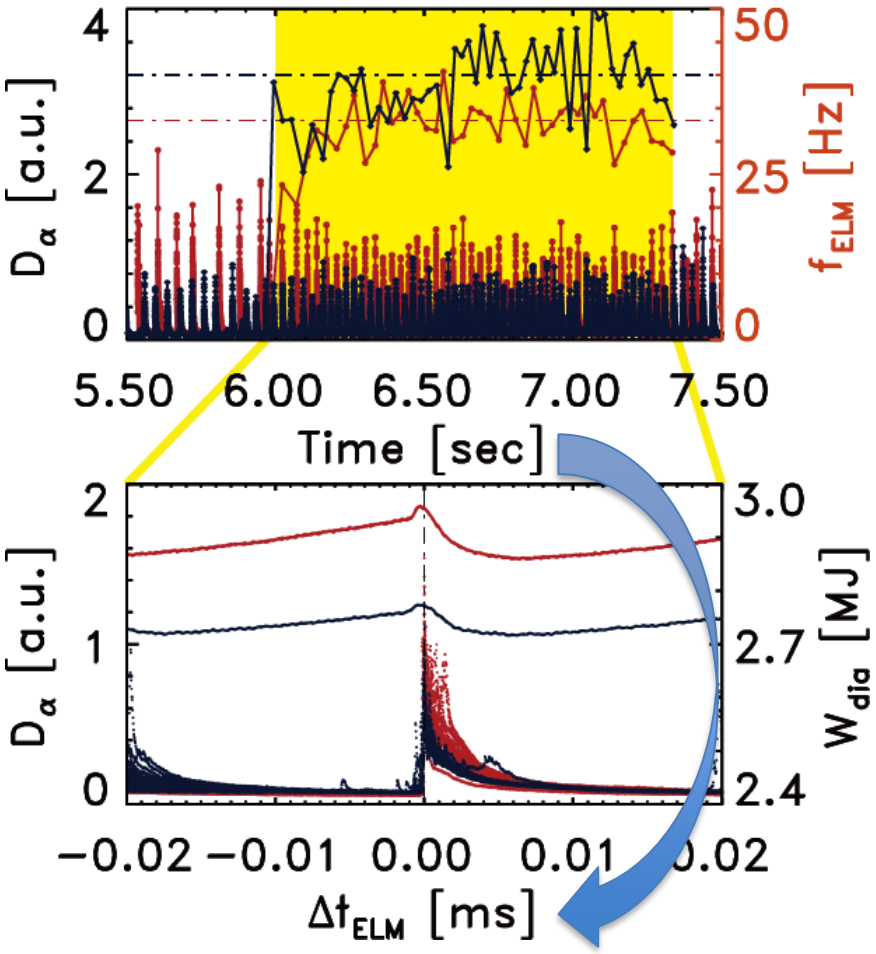

By mapping of multiple, reproducible ELM cycles onto a single time basis (defined by relative time to the ELMs, Δt_{ELM}).

Spatio-temporal structure of ELM perturbation in a variety of momentum input conditions

- Pre-ELM event, E_r profile exhibits a fairly deep well near the separatrix.
- Immediately after the ELM, E_r across the entire region increases, and E_r shear starts to reform within a few ms (or less) , resulting in the pedestal gradient reformation.

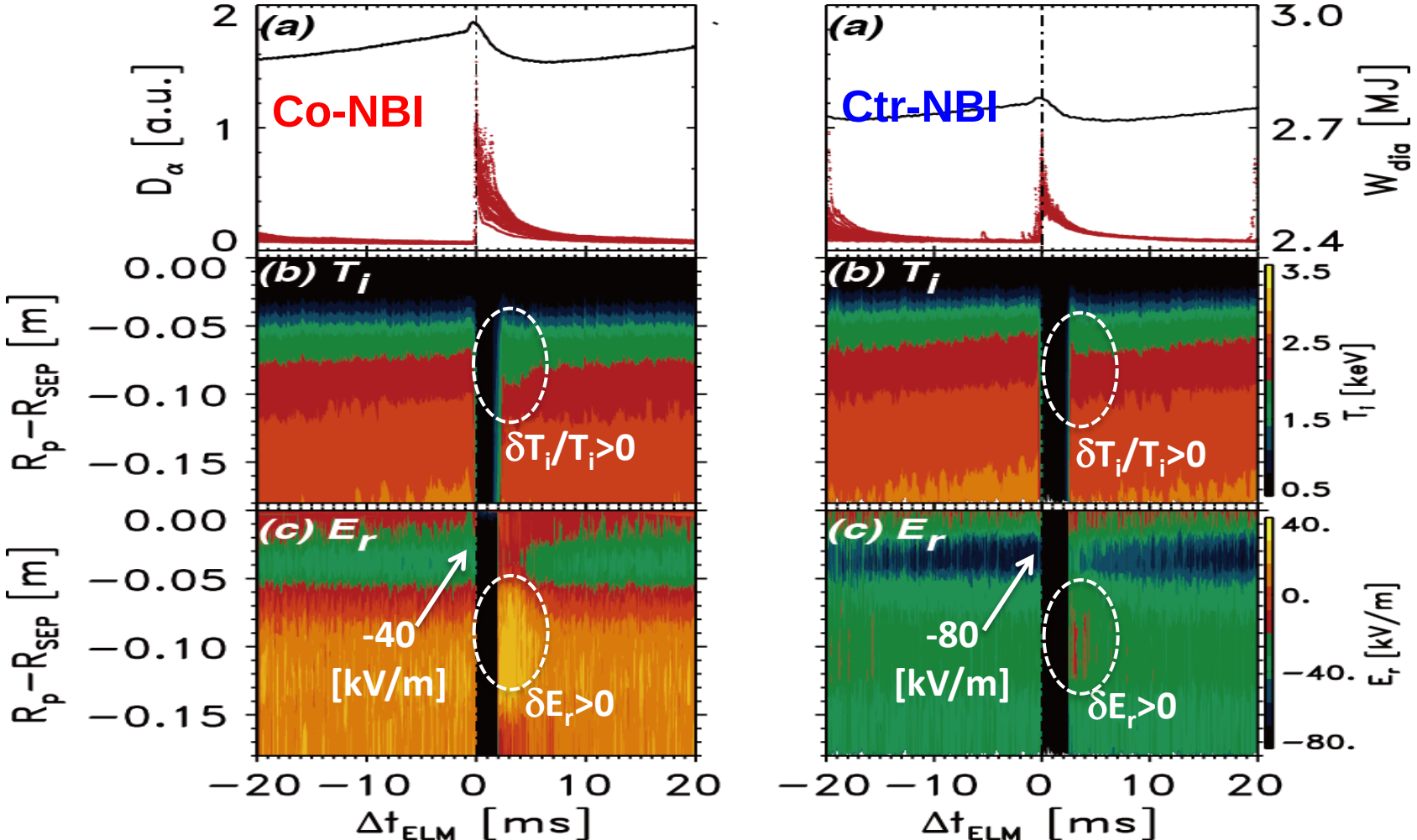

Comparison between pre- and post-ELM stages

Locations for Max. $L_{T_i}^{-1} \equiv -\nabla T_i / T_i$

- There is variation in E_r structure, according to the momentum input directions.
- The Max. normalized gradient (L_{Ti}^{-1}) locations are related to that of E_r-well bottom and/or E_r-curvature-hill, while…
- E_r-shear has local peak values out of them.

The E_r profiles are fitted by parametrized tanh-like functions;

$$E_r(ds) = p(3) + \frac{p(2)}{2}\left\{\tanh\left(\frac{-[ds - p(0)]}{p(1)}\right)\right\}^2 + p(4)\{-[ds - p(0) + p(1)]\}^2$$

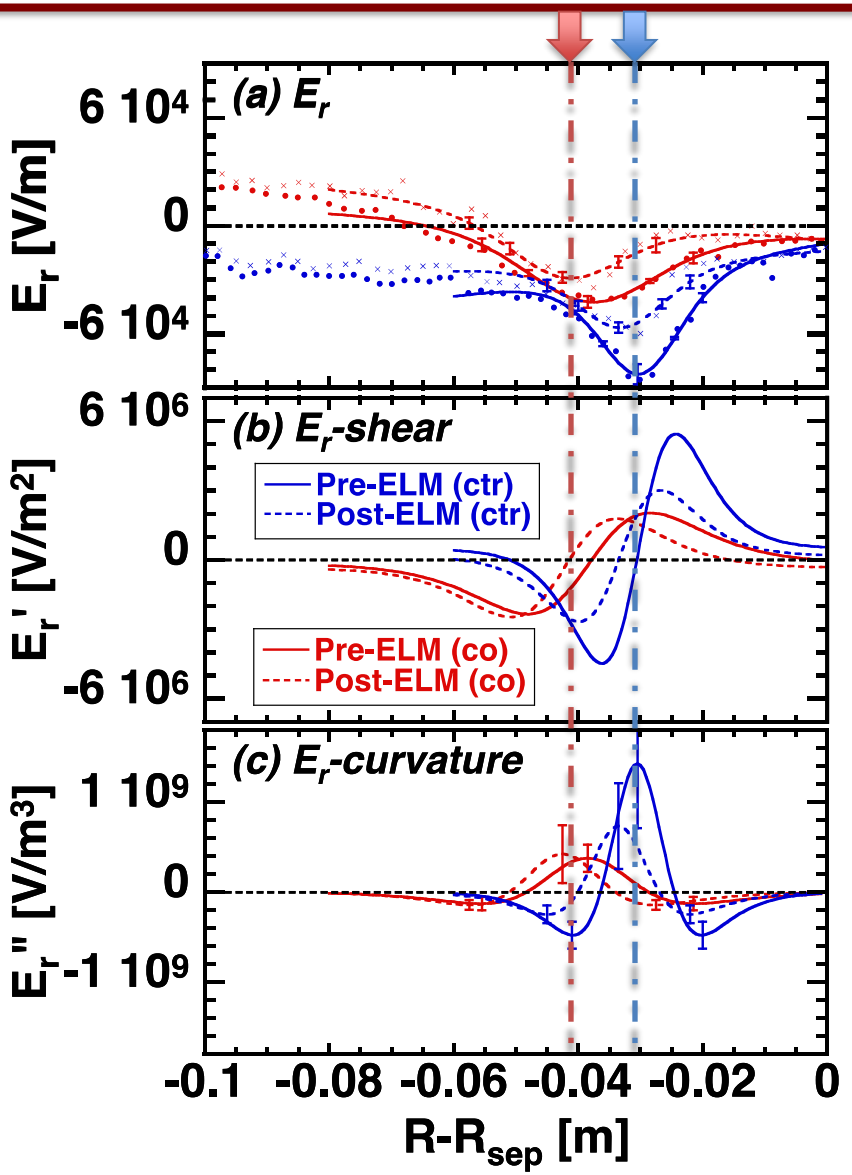

Relationship between the Max. normalized temperature gradient and E_r (and/or E_r") locations

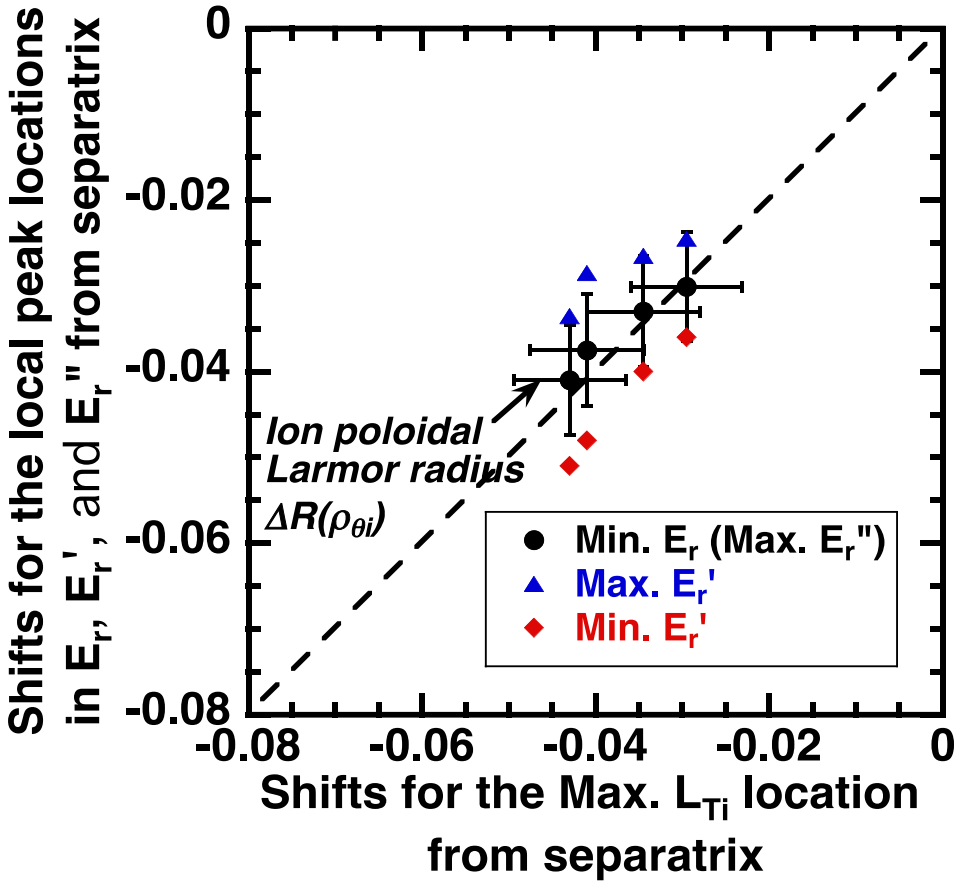

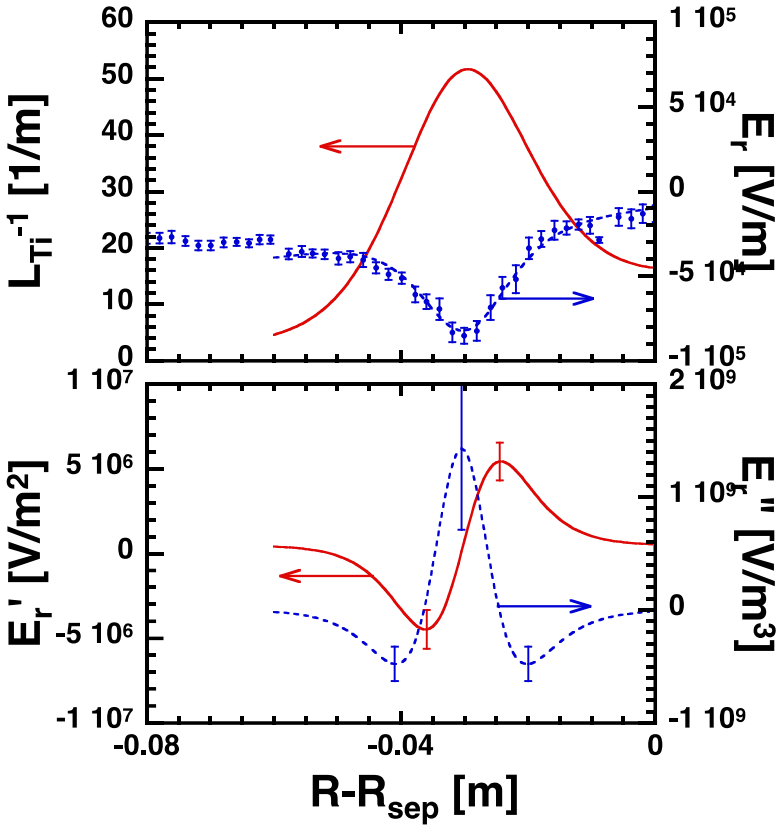

Separation of E_r-shear locations for both positive and negative values is about $\rho_{\theta i}$ (or more) => So that we could discuss on the effect of curvature in a range of spatial resolution of CXRS diagnostics (~ 1cm).

Discussion: The E_r-shear stabilization effects ($\propto E_r' E_r'$) should have a ***double hump*** structure, but it has never been observed in the pedestal profiles

- The sign in E_r' (*i.e. positive or negative shear*) can change when E_r structure has a local peak value (regardless of the sign in E_r).
- As well as experimental observations so far, multi-hump structure (ITB) have never been reproduced. [*Villard, NF 2004*]

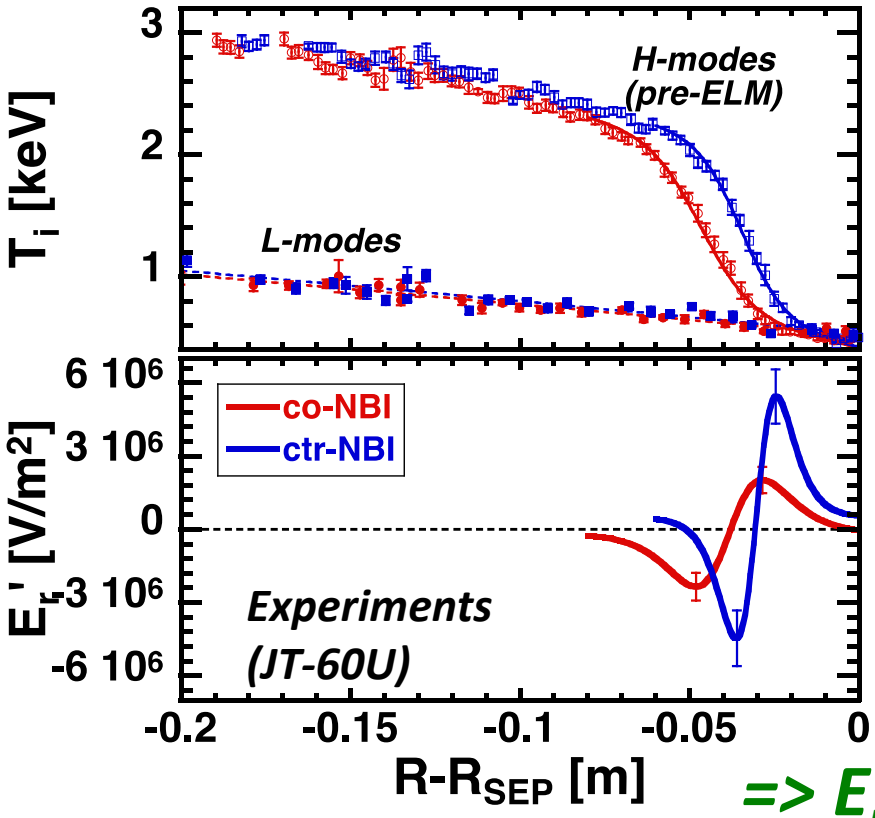

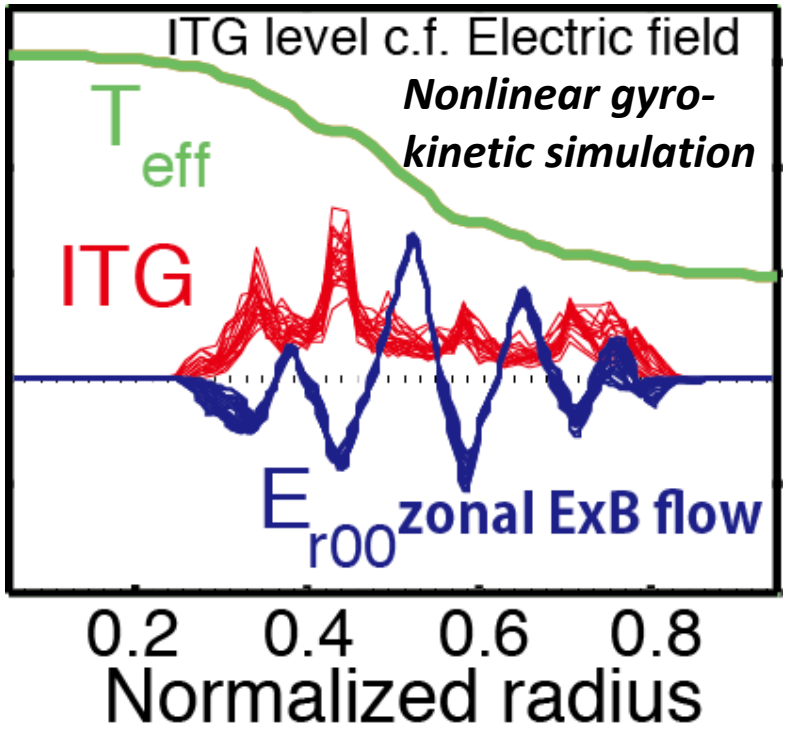

=> E_r-curvature effects ($\propto E_r E_r''$)

Scaling relations of the solitary structure in the edge electric field have been developed

[K. Itoh, et al., Plasma Phys. Control. Fusion 57 (2015) 075008]

	$-E_r E_r''$	E_r	l
Tokamak (plateau regime)	$\frac{1}{\varepsilon_t^2 \rho_p^2}\left(\frac{T_i}{e\rho_p}\right)^2$	$\frac{T_i}{e\rho_p}$	$\varepsilon_t \rho_p$
Tokamak (banana regime)	$\frac{\omega_t}{\nu_i}\frac{1}{\rho_p^2}\left(\frac{T_i}{e\rho_p}\right)^2$	$\frac{T_i}{e\rho_p}$	$\sqrt{\frac{\nu_i}{\omega_t}}\rho_p$
Helical	$\frac{1}{S^2}\frac{1}{\varepsilon_t^2\rho_p^2}\left(\frac{T_i}{e\rho_p}\right)^2$	$\frac{1}{S}\frac{T_i}{e\rho_p}$	$\varepsilon_t \rho_p$

(characteristic value for the width of the peaked profile)

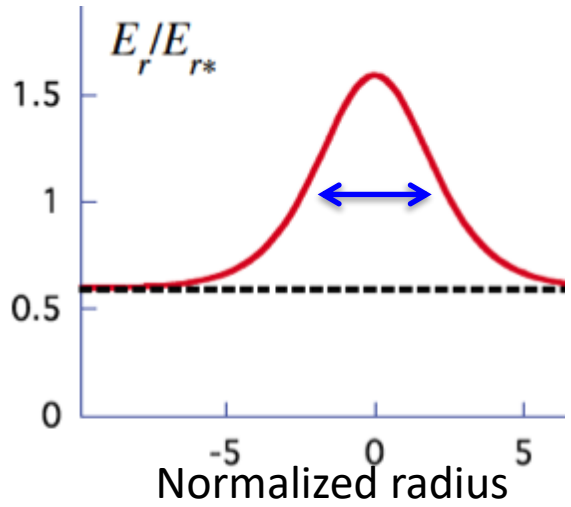

An order of magnitude estimate of the E_r in the experimental units:

Basic equation: $\frac{\partial}{\partial t}E_r = \nabla \cdot \mu_i \nabla E_r - \frac{1}{\varepsilon_0 \varepsilon_\perp}(J_r - J_{\text{ext}})$.

Boundary condition: $X = X_A$ and $dX/dx \to 0$ at $|x| \to \infty$

Non-linear conductivity: (bulk viscosity) $J_r(E_r) = \frac{e n_i \rho_p r}{BR^2}\frac{1}{\sqrt{\pi}}\text{Im}Z(X + i\nu_i\omega_t^{-1})(E_r - E_{r,a})$

Appendix A. Curvature of radial electric field

[K. Itoh, et al., Plasma Phys. Control. Fusion 57 (2015) 075008]

- The curvature of Er is focused upon in considering the suppression of microscopic fluctuations via modulational coupling.
- The turbulent Reynolds stress is proportional to the gradient of the radial electric field, when it is induced by the microscopic fluctuations via disparate-scale interaction;

$$\langle \tilde{v}_r \tilde{v}_\theta \rangle \propto \frac{\mathrm{d}}{\mathrm{d}r} E_r$$

- This is natural from symmetry consideration. Thus, the force by this Reynolds stress per unit mass density is proportional to the curvature of the radial electric field. The power absorbed from turbulence by the flow is proportional to the force multiplied by velocity and has a relation;

$$V_{\mathrm{E\times B}} \frac{\mathrm{d}}{\mathrm{d}r} \langle \tilde{v}_r \tilde{v}_\theta \rangle \propto -E_r \frac{\mathrm{d}^2}{\mathrm{d}r^2} E_r$$

- Therefore, the product of electric field and its curvature, XX" in normalized variable, has a key role in the suppression of turbulence via modulational coupling.

An order of E_rE_r" predicted by model is not far from experimental observations

JT-60U (ELMy H-modes): E_rE_r"≈$10^{13\sim14}$ [V^2/m^4]. *Kamiya, PoP2014*

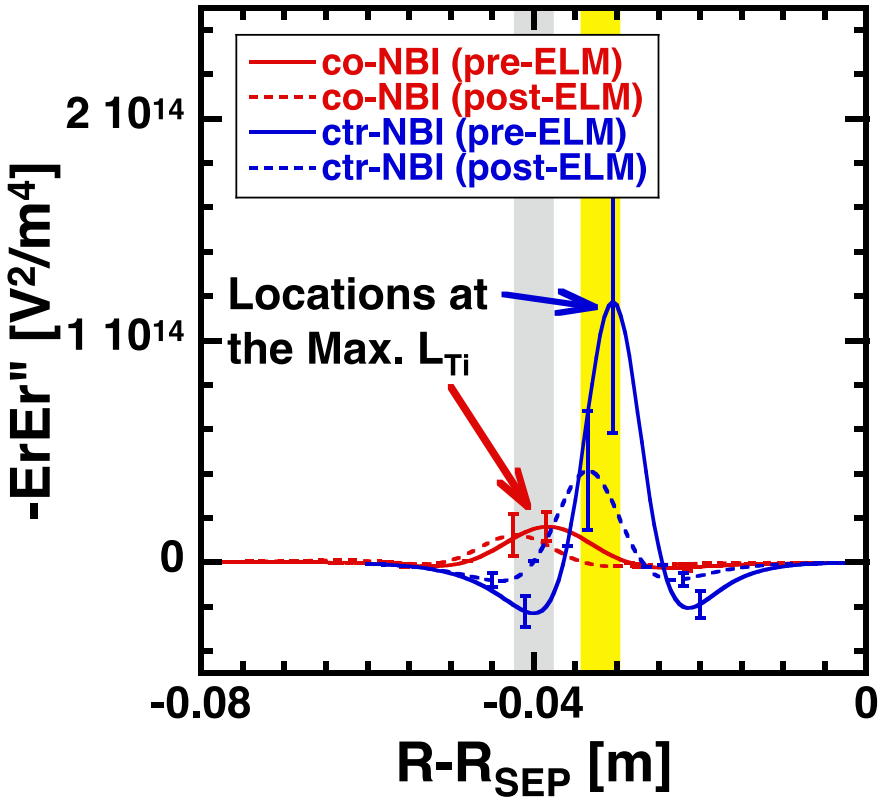

$$-E_rE_r'' \simeq \frac{1}{S^2}\frac{1}{\varepsilon_t^2\rho_p^2}\left(\frac{T_i}{e\rho_p}\right)^2 \cdot \quad S \simeq \frac{7.5}{Mq\sqrt{2\varepsilon_h}}\frac{1}{\nu_{*,h}}$$

LHD (electrode biasing): ErEr"≈10^9 [V^2/m^4]. *Tokuzawa, PoP2014*

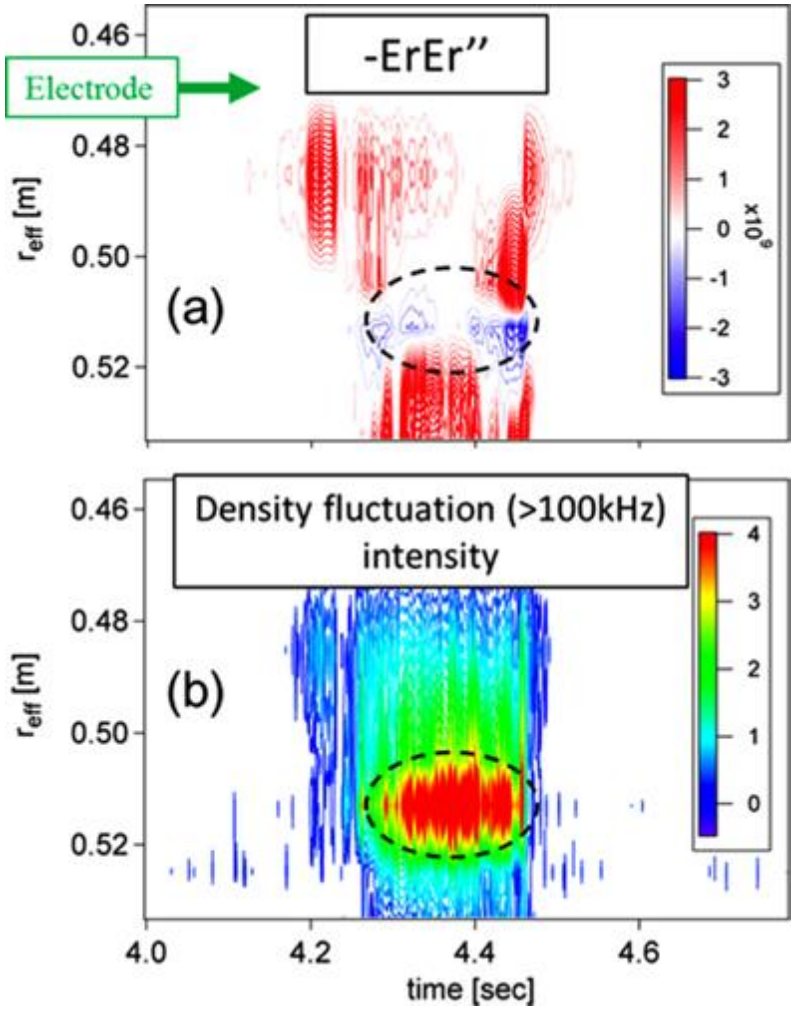

Concentration of turbulence intensity is correlated with $E_r E_r$"

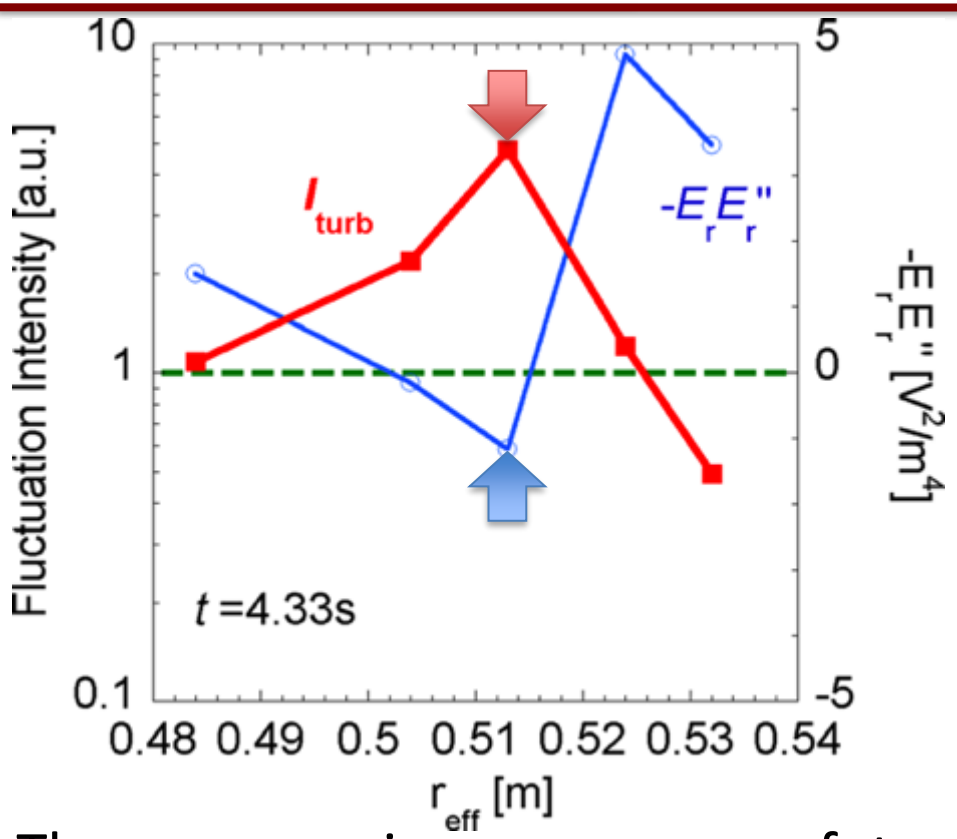

These comparisons *encourage* future experimental test of the bifurcation model, by comparing the time-scale of transition, to the observation in the relevant tokamak experiments.

LHD (electrode biasing): ErEr"≈10^9 [V^2/m^4].

Tokuzawa, PoP2014

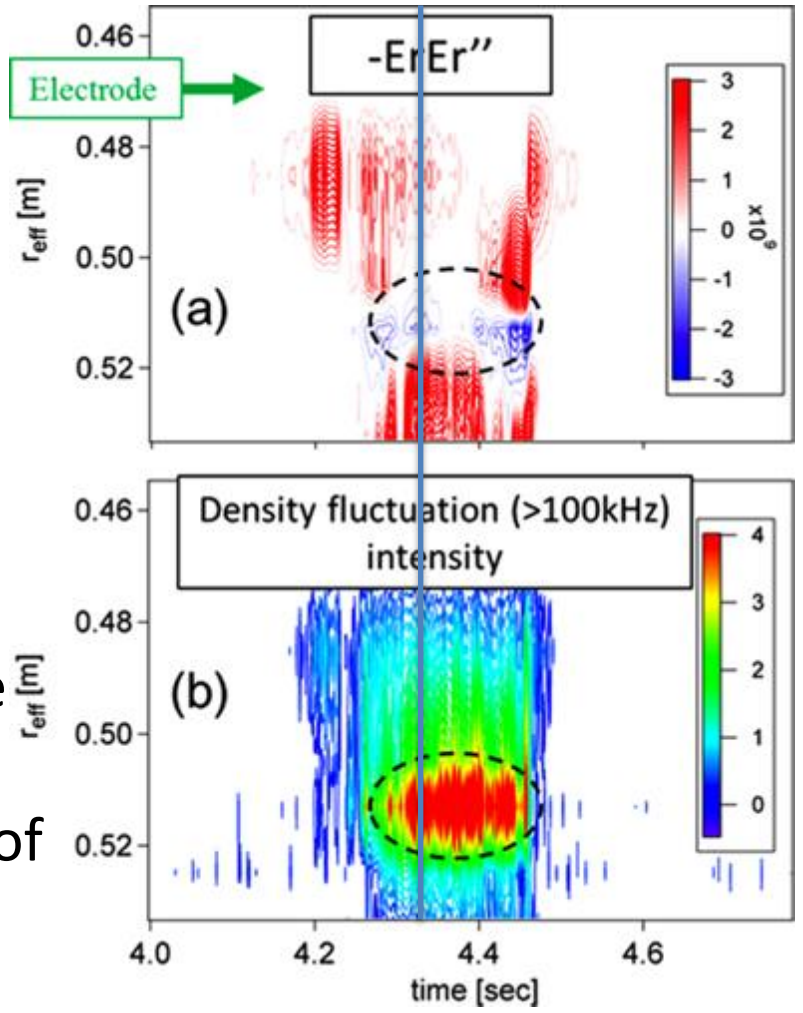

But, "*causality*" is still unknown for a transient phenomena

Complex multi-stage E_r transition during ELM-free (Kamiya, PRL 2010)

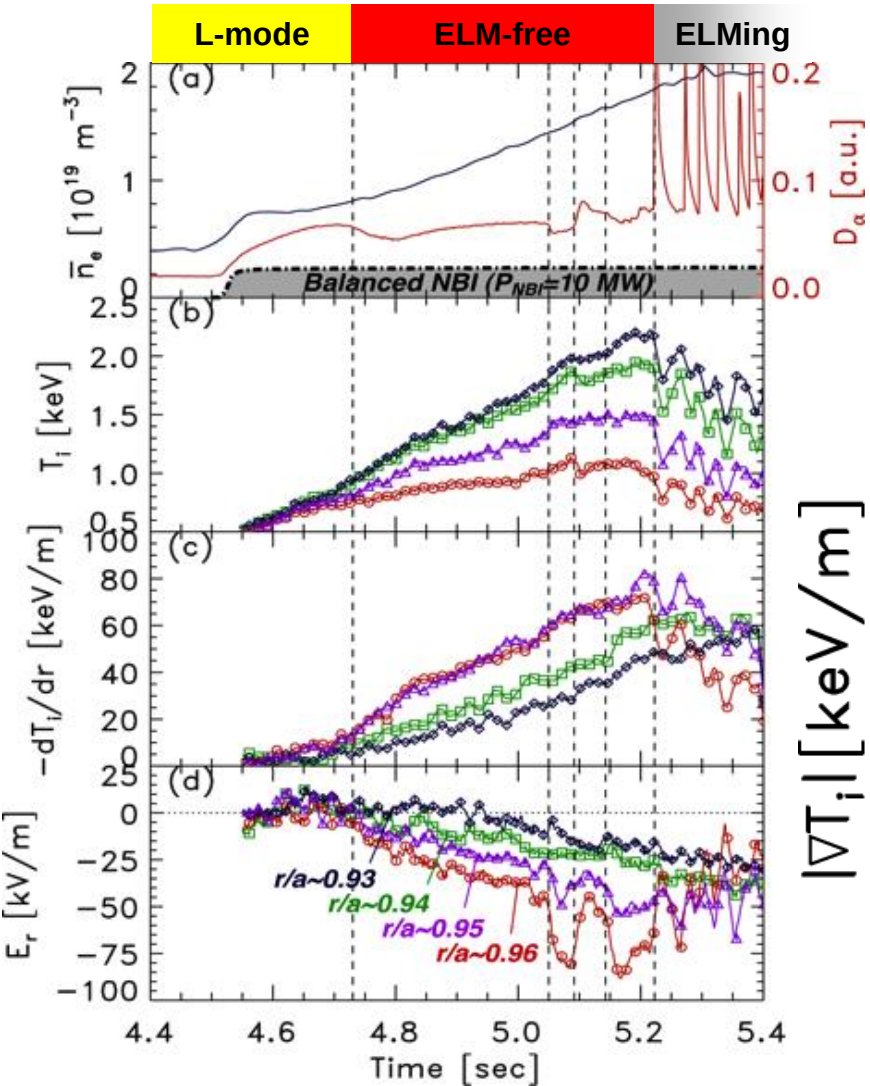

1) Mean E_r can deviate from grad-p term during a "slow" L-H transition with formation of a shallow E_r-well structure.

2) E_r jumps to a larger value during EF-phase with a almost developed pedestal, while the T_i gradient does not change much simultaneously. =>> Why?

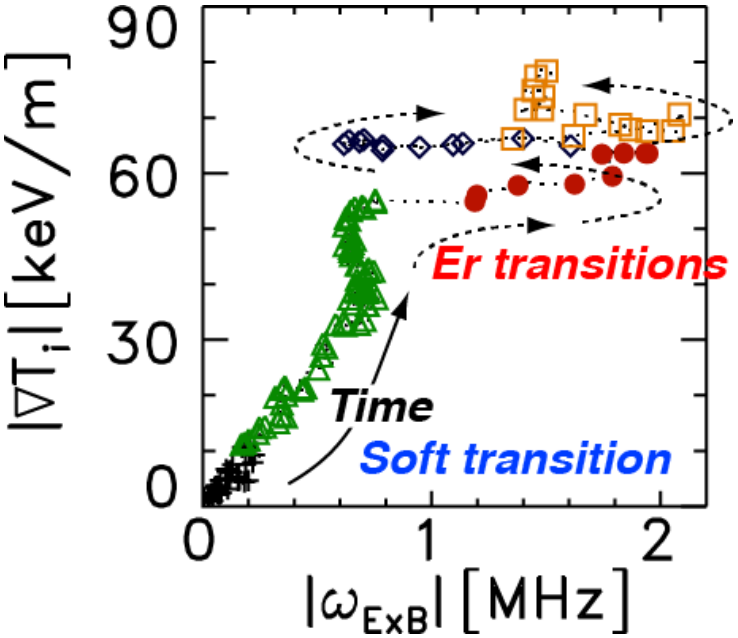

ExB shearing rate:

$$\omega_{ExB} = \frac{r}{q}\frac{d}{dr}\left(\frac{q}{r}\cdot\frac{E}{B}\right)$$

[T. S. Hahm, PoP1994]

T_i pedestal may not necessarily be followed by the change in the E_r structure, especially for a later H-phase

Both weak and strong E_r phases seem to be *quasi-stable*

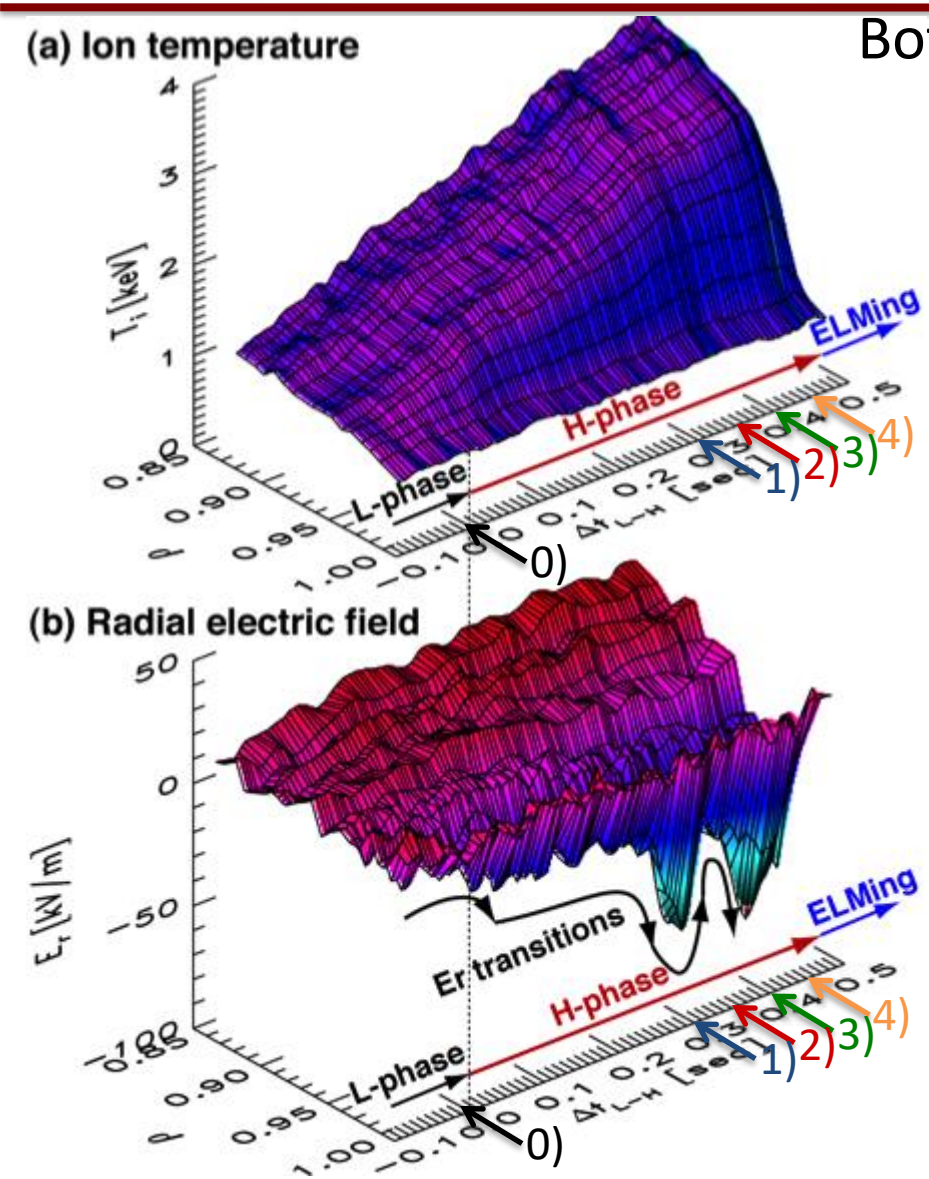

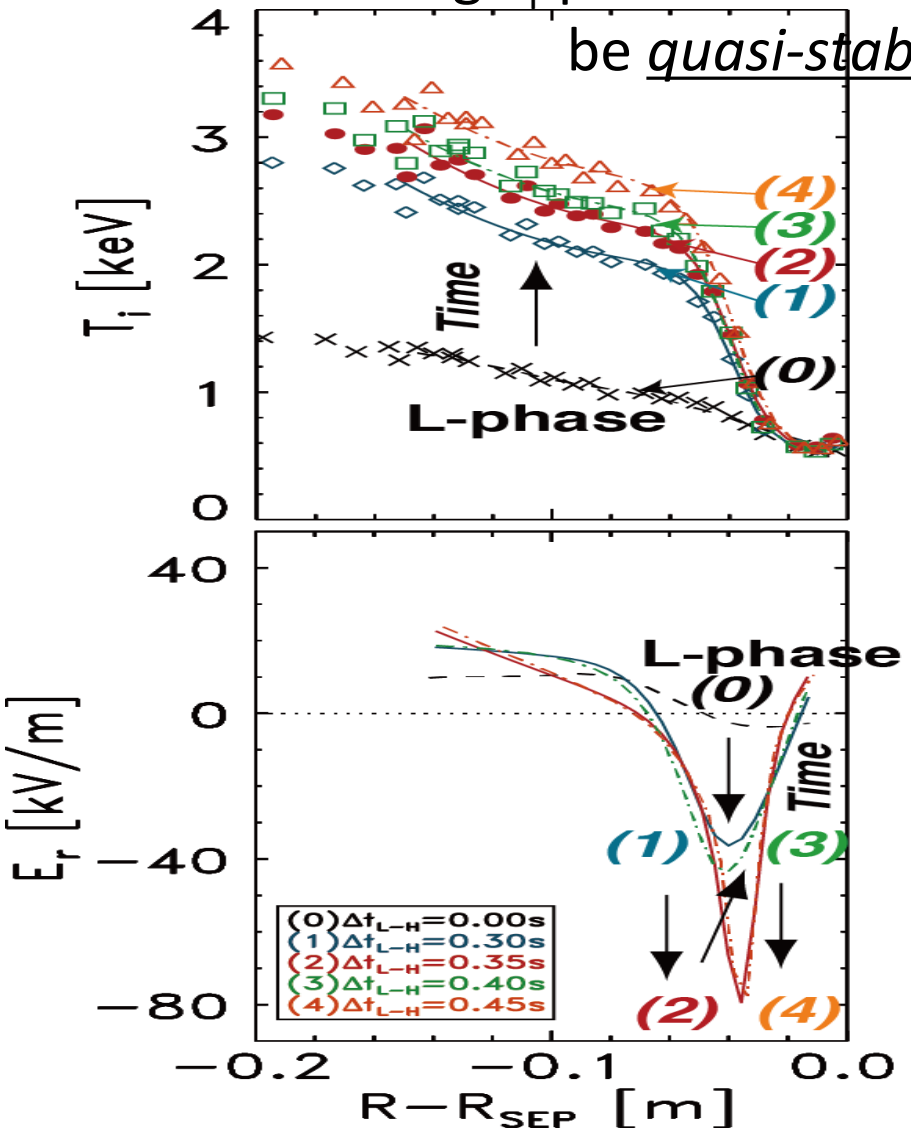

Replacement of ZF (GAM) to MF
may not direct cause for the L-H transition

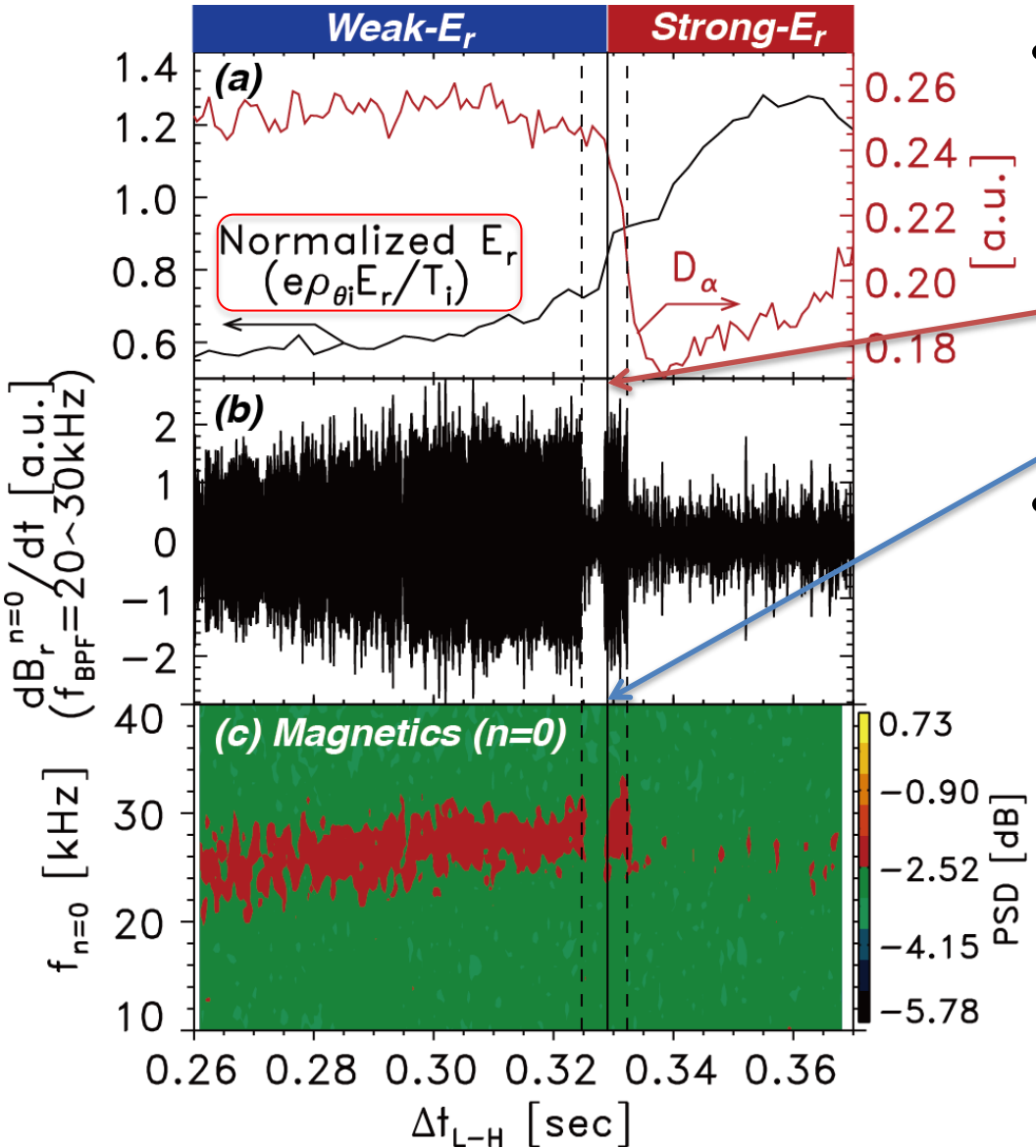

- Across the "fast" transition during ELM-free phase, E_r-bifurcation occurs ***at normalized E_r value ~1*** in association ***with n=0 fluctuation (GAM).***
- *The exact causality is NOT very well understood*, although the phenomenology of this "replacement" is rich and complex for theoretical studies.

Summary and future direction

- We revisited the studies of *paradigm* of shear suppression of turbulence as the mechanism for the edge transport barrier formation with an improved diagnostic.
  - Spatiotemporal structures of the LCO and causal relation among E_r, gradient, and turbulence by using a HIBP (JFT-2M ~FY2004).
  - Relationship among pedestal gradient and E_r structure (including its shear and curvature) by using a CXRS (JT-60U ~FY2008).
- These new findings shed light on the underlying physics mechanism in the turbulent toroidal plasmas, supporting E_r bifurcation model partially.
- A more detailed comparison between experiment and model will be left for a future investigation.

Acknowledgement

- This work was performed under a collaboration between JAEA, NIFS, and Kyushu-university.
- Special thanks goes to Prof. K. Itoh and Prof. S. -I. Itoh for their continuous encouragement.
- Also Drs. T. Ido and T. Kobayashi for their contributions of JFT-2M HIBP measurements.

References

1. F. Wagner, et al. Phys. Rev. Lett. **49**, 1408 (1982).
2. ASDEX Team, Nucl. Fusion **29**, 1959 (1989).
3. H. Matsumoto, et al., Nucl. Fusion **27**, 1181 (1987).
4. S. -I. Itoh, and K. Itoh, Phys. Rev. Lett. **60**, 2276 (1988).
5. K. C. Shaing and E. C. Crume, Jr., Phys. Rev. Lett. **63**, 2369 (1989).
6. R. j. Groebner, et al., Phys. Rev. Lett. **64**, 3015 (1990).
7. K. Ida, et al., Phys. Rev. Lett. **65**, 1364 (1990).
8. R. J. Taylor, et al., Phys. Rev. Lett. **63**, 2365 (1989).
9. T. Ido, et al., Phys. Rev. Lett. **88**, 055006 (2002).
10. T.E. Stringer, Phys. Rev. Lett. **22**, 1770 (1969).
11. R.D. Hazeltine, et al., Phys. Fluids **14**, 361 (1971).
12. N. Winsor, et al., Phys. Fluids 11, 2448 (1968).
13. K. H. Burrell, Plasma Phys. Control. Fusion **34**, 1859 (1992).
14. K. H. Burrell, Phys. Plasmas **4**, 1499 (1997).
15. K. Ida, Plasma Phys. Control. Fusion **40**, 1429 (1998).
16. Y. Miura, et al., Phys. Rev. Lett. **69**, 2216 (1992).
17. W. Herrmann and ASDEX Upgrade Team, Phys. Rev. Lett. **75**, 4401 (1995).
18. T. N. Carlstrom and R. J. Groebner, Phys. Plasmas **3**, 1867 (1996).
19. K. Itoh and S. -I. Itoh, Plasma Phys. Control. Fusion **38,** 1–49 (1996).
20. F. L. Hinton, et al., Phys. Rev. Lett. **72**, 1216 (1994).
21. P. H. Diamond, et al., Phys. Rev. Lett. **72**, 2565 (1994).
22. E. J. Kim and P. H. Diamond, Phys. Rev. Lett. **90**, 185006 (2003).
23. P. H. Diamond, et al., Plasma Phys. Control. Fusion **47**, R35–R161 (2005).
24. G. D. Conway, et al., Phys. Rev. Lett. **106**, 065001 (2011).
25. G.R. McKee, et al., Nucl. Fusion **49**, 115016 (2009).
26. T. Kobayashi, et al., Phys. Rev. Lett. **111**, 035002 (2013).
27. T. Kobayashi, et al., Nucl. Fusion 54, 073017 (2014).
28. K. Kamiya, et al., Phys. Plasmas **21**, 122517 (2014).
29. T. S. Hahm, et al., Phys. Plasmas **1**, 2940 (1994)
30. T. Tokuzawa, et al., Phys. Plasmas **21**, 055904 (2014).
31. K. Kamiya, et al., , Phys. Rev. Lett. **105**, 045004 (2010).